# Real time damage detection using recursive principal components and time varying auto-regressive modeling

M.Krishnan

*Graduate student, Department of Civil Engineering, Indian Institute of Technology, Guwahati, Assam, India*

B.Bhowmik

*Doctoral student, Department of Civil Engineering, Indian Institute of Technology, Guwahati, Assam, India*

B.Hazra*

*Assistant Professor, Department of Civil Engineering, Indian Institute of Technology, Guwahati, Assam, India*

V.Pakrashi*

*Assistant Professor, School of Mechanical & Materials Engineering, University College Dublin, Belfield, Ireland*

**Abstract**

In this paper, a novel baseline free approach for continuous online damage detection of multi degree of freedom vibrating structures using Recursive Principle Component Analysis (RPCA) in conjunction with Time Varying Auto-Regressive Modeling (TVAR) is proposed. In this method, the acceleration data is used to obtain recursive proper orthogonal components online using rank-one perturbation method, followed by TVAR modeling of the first transformed response, to detect the change in the dynamic behavior of the vibrating system from its pristine state to contiguous linear /non-linear-states that indicate damage. Most of the works available in the literature deal with algorithms that require windowing of the gathered data owing to their data-driven nature which renders them ineffective for online implementation. Algorithms focussed on mathematically consistent recursive techniques in a rigorous theoretical framework of structural damage detection is missing, which motivates the

☆Fully documented templates are available in the elsarticle package on CTAN.

*Corresponding author

*Email address:* budhaditya.hazra@iitg.ernet.in (B.Hazra)

development of the present framework that is amenable for online implementation which could be utilized along with suite experimental and numerical investigations. The RPCA algorithm iterates the eigenvector and eigenvalue estimates for sample covariance matrices and new data point at each successive time instants, using the rank-one perturbation method. TVAR modeling on the principal component explaining maximum variance is utilized and the damage is identified by tracking the TVAR coefficients. This eliminates the need for offline post processing and facilitates online damage detection especially when applied to streaming data without requiring any baseline data. Numerical simulations are performed on a 5-dof nonlinear system under white noise and El Centro excitations, with different levels of nonlinearity simulating the damage scenarios, demonstrate the robustness of the proposed algorithm. The method is further validated on results obtained from case studies involving experiments performed on a cantilever beam subjected to earthquake excitation; a two-storey bench-scale model with a TMD and, data from recorded responses of UCLA factor building demonstrate the efficacy of the proposed methodology as an ideal candidate for real-time, reference free structural health monitoring.
*Keywords:* Recursive Principal Component Analysis (RPCA), Time-Varying Autoregressive Modeling (TVAR), Damage Sensitive Features (DSF)

---

## 1. Introduction

Structural damage detection involving condition assessment, fault diagnosis and prognosis of civil, mechanical and aerospace infrastructure has garnered significant attention and a wealth of literature exists in this area ([1, 2, 3, 4]). Largely premised on the idea that damages manifest themselves through the alteration of structural dynamic properties such as natural frequency, modeshapes, damping; a significant number of algorithms and methodologies have been proposed in recent times ([5, 6, 7, 8, 9, 10, 11]). Damages mostly occur due to higher operational loads, excessive response, propagation of cracks, buckling, fatigue, impact of a foreign object, etc. An ideal damage detection framework should provide detection in near real time, identify the presence of damage and its location and estimate the severity of the damage in the structure. Currently available damage detection schemes ([7, 8, 9, 10]) are mostly offline in nature and data processing usually happens in batch mode; hence, the development of online damage detection techniques based on processing of response

that streams in real-time, still remains a challenge. Traditional offline damage detection schemes have disadvantages mostly due to their inherent dependence on finite element modeling, restriction in the evolution of a universal methodology for damage detection in various structures and their insensitivity towards initial tiny damages in structures. Recursive implementation of the existing damage detection algorithms ([12, 13]) are computationally expensive and mathematically complex which motivates the need for an online framework that enables the selection of the feature index of structural damage very flexible. This paper proposes a real time damage detection framework using time varying auto regressive (TVAR) ([14]) modeling in conjunction with recursive principal component analysis (RPCA) ([15]), to detect spatio-temporal structural damage in real time.

A vast majority of the developed damage detection techniques are global in nature, i.e., the dynamic or modal properties are obtained for the entire structure from the input-output data using global structural analysis ([8, 9, 10, 16]). Successful application of system identification-based SHM techniques require good quality data acquired using a dense sensor network and an extensively calibrated finite element model (FEM) ([16, 17, 18]); thus rendering them computationally expensive and cumbersome. The need for an accurate finite element (FE) model, accounting for modeling errors, choice of tunable parameters, limit their applications towards real time damage detection. The response based methods mostly entails a close monitoring of the structure over time using periodic measurements, extraction of damage indicators or damage-sensitive features (DSF) from the measurements, followed by a extensive statistical pattern classification based approach to depict the present state of the system health. These response based methods mostly rely on the signatures obtained from the recorded vibrations to extract features that indicate a change at the onset of damage. Recent developments in the response based detection exploits classical time-frequency analysis such as wavelet transform ([9, 19, 20]), empirical mode decomposition, Hilbert Huang transform ([21, 22]) and blind source separation ([10, 23, 24]).

Data driven statistical techniques (such as Principal Component Analysis (PCA)) utilize the eigen subspace of the system obtained from the eigen value decomposition of the response covariance matrix for detecting damage, thus enabling the monitoring of complex systems with less computational load ([25, 26, 27]). The eigen space characteristics of a system can be used to track global information about time varying parameters

(i.e., frequency, damping and mode shape) in order to detect changes in a structure's health over time. Statistical measures like root mean square deviation and Welchs t-test ([25]), applied on the principal component loadings obtained from response signals, scatter plots of pre and post damage principal components (PCs) derived from application of PCA on transmissibility function, PCA in combination with multivariate statistical inference ([26, 28]), are some of the examples for application of PCA in damage detection and system identification applications ([11, 29, 30]). However, PCA is heavily reliant on the use of baseline data which could potentially inhibit its application in online damage detection. This underscores the need of recursive damage detection techniques. Recursive subspace identification ([12, 13]), recursive least-squares based identification algorithms([31]), hybrid clustering and least squares algorithm for nonlinear systems using radial basis function networks([32]), detection of change points in data using CUSUM ([33, 34]) are some notable contributions in the context of adaptive/recursive system identification. However, the recursive identification techniques have found limited applicability towards realtime damage detection in recent times to due algorithmic complexities.

Most of the works are based on application of algorithms that are applied on windowed data ([26, 30]). These algorithms are data driven, computationally intensive and mathematically complex, which prompts the need to adapt an online implementation with less computational exhaustion and a greater flexibility in extracting feature index of structural damage from a set of physical response. The main motivation behind the present work is to develop a novel damage detection framework which can process the data online and to detect damages in the structure in real time. In most of the practical structural health monitoring scenarios, data streams in continuously in real-time in both longer and/or shorter monitoring durations. Thus any damage detection algorithm should ideally work online, which further necessitates that it should be parameter and baseline free. This motivates the utilization of the concepts of RPCA ([15]), providing a recursive update of eigen subspace, as a tool for real time processing of data in the present work. Whereas most of the PCA based techniques process batches of data acquired in batch mode over a certain period of time, RPCA provides online processing of data based on rank one eigenvector updates in a recursive framework, as and when the data streams in. A major requirement for the working of the RPCA algorithm is that the data covariance matrix should be strictly diagonally dominant at any instant of time, which is automatically satisfied for structural dynamical systems having low to moderate damping. Once the eigen space updates are obtained, the proposed framework utilizes

time-varying auto-regressive (TVAR) ([14]) modeling in conjunction with damage sensitive features (DSFs) for identifying the instant of damage.

An autoregressive (AR) process may be used to model activity that is generated by one or more superimposed responses, operating under the premise that past values obtained from a time series affects the current values, based on some statistical calculations ([35]). The primary advantage of the AR model is that the underlying process that produces the observed data can be inferred directly from the AR parameters without resorting to spectral representation. Time series models work extremely well in capturing the key features of any data series. Literature utilizing time series modeling for damage detection is quite extensive ([1, 6, 24, 36, 37]) but with the disadvantage that basic AR modeling is not amenable for online implementation. To tailor AR modeling towards recursive implementation and to better capture the non-stationarity involved with any data or due to the damage induced, TVAR modeling was proposed ([10, 14]). However, a major concern for using the TVAR models is pre-selection of the model order. In the proposed method, TVAR modeling is applied on the transformed responses obtained from the RPCA algorithm rather than the raw vibration responses. Therefore, relatively low model order of time-series model ([10, 38]) is sufficient to capture the dynamics of the structure in the transformed domain. The online damage detection framework, exclusive of baseline data, is used to identify the damage instant in the monitored system through the time varying coefficients of the TVAR models. In the proposed framework, damages in structures can be detected both spatially and temporally in real-time.

The major contributions of this work are as follows: **First**, a novel framework has been provided using RPCA as an online damage detection tool that works in real time as data is continuously gathered. To the best knowledge of the authors, the aspect of using RPCA in the context of structural damage detection has so far not been explored. **Second**, the use of TVAR model on the transformed responses from which damage can be inferred using DSFs even for 15% global damage, is a novel idea that is proposed in this paper, which provides a greater degree of damage detection than currently reported in the literature. **Third**, simultaneous spatial and temporal descriptions of damage is difficult and the key entitlement of this work is to detect spatio-temporal damage in real time. To this extent, spatio-temporal damage detection for local stiffness changes up to 25% is accomplished in this paper. **Finally**, the paper also explores the possibility of applying the proposed algorithm

for under-determined scenarios as well where the number of sensors is less than the number of degrees of freedom. The non stationary nature of the input data is taken into account by applying higher order statistical moments in order to identify the instant of damage. The proposed method is applied for damage detection in a 5 degree of freedom (dof) buocwen system excited with white noise and 1940 El Centro earthquake ground motion, in which the nonlinearity level is subjected to various degrees of changes to simulate different levels of damage in the structure. These numerical results were complemented with experimental tests on a shake table using an aluminium cantilever beam, in which nonlinearity is induced with a thin rubber strip attached to the free end of the beam. Important conclusions are also drawn from a case study involving a two-storey bench-scale model with a TMD, in which the change of state from de-tuned to tuned is detected by the algorithm.

The paper is organized as follows. First, a brief description of RPCA is presented in the framework of structural dynamics. The damage detection through the use of DSF is presented next. The proposed algorithm is demonstrated with the aid of numerical examples. Finally, the results are presented using experimental setups carried out in a lab environment to demonstrate the efficiency and robustness of the proposed algorithm in practical situations. The experimental results are also complemented through a full-scale study of the UCLA factor building under a combination of earthquake and ambient data.

## 2. Background

PCA, also known as *Karhunen-Loève* transform, can be applied for dimensionality reduction, lossy data compression, feature extraction and data visualization ([29]). PCA can be defined as the orthogonal projection of the data onto a lower dimensional linear space, known as the *principal subspace*, such that the variance of the projected data is maximized ([39]). By reducing the a complex data set to a lower dimension, PCA reveals some simplified structures relevant to the data set which could be extracted using eigen value decomposition (EVD) on the sample covariance matrix. This decomposition produces the eigen value matrices,expressible as time series waveforms, known as the *principal orthogonal values* (**POVs**) and eigen vector matrices, also known as *proper orthogonal matrices* (**POMs**). Eigen values/POVs describe the relative significance of each POM in the response as a whole. The uncorrelated new set of variables produced by the linear combinations

of the original variables are known as the *principal orthogonal components* (**POCs**). The new set of variables have an improved potential to detect deviations (such as structural damage) in the system as compared to the original set of variables and hence, finds its way in the field of structural damage detection.

Traditional PCA based methods analyze data in a batch mode, offline. As PCA is a baseline reliant approach, the analyzed data are windowed so as to compare it with reference over certain intervals of time. Practical engineering applications require the choice of window parameters such as window size, shift, overlap, etc. to be discrete and problem specific. For applying the concept of PCA for incorporating non-linear dependence between variables, a variation of PCA, known as kernel PCA (KPCA)([40]) is sometimes utilized to account for the presence of nonlinearities in the data in the context of damage detection. However, KPCA based approaches relying on the concept of subspace angle is computationally expensive. The pith of any PCA analysis is the EVD of the sample covariance matrix to obtain eigenvalues and eigenvectors, but for a real time framework, applying EVD at each time instant is cumbersome. To alleviate this drawback, a baseline free approach amenable to online damage detection is addressed by the RPCA based framework ([15]). The eigenspace of the sample covariance matrix applied to the data vector is updated recursively using the rank-one update which provides an immediate estimation of the eigenvalue and the eigen vector matrices, instead of updating the covariance matrix directly. An initial covariance estimate for the first few seconds is essential to attune the basic RPCA towards online damage detection is proposed in this paper which provides an efficient framework to detect damage online.

### *2.1. RPCA and structural dynamics*

In order to understand the application of RPCA in the purview of structural dynamics, consider a linear, classically damped, and lumped parameter system with mass, stiffness and damping matrices **M**, **C** and **K** subjected to an external force, with **x** as the displacement vector.

$$[\mathbf{M}]\{\ddot{x}(t)\} + [\mathbf{C}]\{\dot{x}(t)\} + [\mathbf{K}]\{x(t)\} = \{\mathbf{F}(t)\} \tag{1}$$

where $\mathbf{F}(t)$ is the input excitation which is assumed to be Gaussian and broadband. The solution of the equation can be written as

$$\{\mathbf{x}\}_m = [\mathbf{V}]_{m\times s}\{\mathbf{q}\}_s \tag{2}$$

where $\mathbf{x}$ is the measurement matrix of size $m \times N$, $\mathbf{q}$ is the matrix of corresponding modal coordinates of size $s \times N$. Here $m$ represents the number of degrees of freedom and $s$ is the number of modes considered with $N$ as the sampling size. $[\mathbf{V}]_{m\times s}$ is the mode shape matrix which transforms the data from modal coordinates to the physical response. An important characteristics of the mode shape matrix is that each columns of the mode shape matrix are orthogonal to each other with respect to the matrix $\mathbf{M}$. The covariance matrix of $\mathbf{X}$ can be expressed as

$$\begin{aligned}\mathbf{R} &= \frac{1}{N}\mathbf{X}\mathbf{X}^T \\ &= \frac{1}{N}\mathbf{V}\mathbf{Q}\mathbf{Q}^\mathbf{T}\mathbf{V}^\mathbf{T}\end{aligned} \tag{3}$$

In equation 3, $\mathbf{R_Q} = \frac{1}{N}\mathbf{Q}\mathbf{Q}^\mathbf{T}$ can be identified as the covariance matrix of the modal responses. For undamped free vibration (i.e., $\mathbf{C} = 0$ and $\mathbf{F} = 0$ in equation 1), $\mathbf{R_Q}$ is exactly a diagonal matrix, while under mildly damped forcing conditions (i.e., $\mathbf{C} \neq 0$ and $\mathbf{F} \neq 0$ in equation 1), the matrix $\mathbf{R_Q}$ is an approximately diagonal matrix as the samplesize of the responses increase ([41]). Under broadband excitations, the evolution of the physical response, $\mathbf{x_i(t)}$ and modal response $\mathbf{q_i(t)}$, in time domain can be expressed in terms of the impulse response function as in equation 4.

$$q_i(t) = \int_0^\infty h(t-\tau)\, f_i(\tau)\, d\tau \tag{4}$$

where $\mathbf{f}_i(\tau)$ represent the modal forces, related by the equation $\mathbf{f}_i(\tau) = v_i^T\mathbf{F}_i(\tau)$, where $v_i$ represents the mode shape corresponding to the mode and $\mathbf{F}_i(\tau)$ represent the actual forces. The individual elements of the covariance matrix $\mathbf{R_Q}$ can be expressed as:

$$r_{ij}^Q = \int_{\tau=0}^{\infty}\int_{\theta=0}^{\infty} f_i(\tau)f_j(\theta)\left[\frac{1}{N}\sum_{i,j} h_i(t-\tau)h_j(t-\theta)\right]d\tau d\theta \tag{5}$$

Equation 5 shows that for finitely large N, $\mathbf{R_Q}$ can be expected to be a diagonal matrix for undamped system and nearly diagonal for light to moderate modal damping. The POCs ($\psi$) or orthogonal transformation of the data can be written as product of POMs ($\mathbf{W}$) and the data vector ($\mathbf{x}$) as:

$$\begin{aligned}\psi_i(t) &= \mathbf{W}^{\mathbf{T}} x_i(t) \\ &= (\mathbf{V} + \varepsilon)^T x_i(t) \\ &= q_i(t) + \gamma\end{aligned} \tag{6}$$

Hence POCs ($\psi$) can be expressed as a sum of true linear normal coordinates ($q$) and an error term ($\gamma$). To understand the behavior of covariance matrix of POC, $\mathbf{R_\Psi} = \frac{1}{N}\mathbf{\Psi}\mathbf{\Psi}^{\mathbf{T}}$ its essential to realize the individual elements of the $\mathbf{R_\Psi}$ matrix. Substituting from equation 6,

$$\begin{aligned}r_{ij}^{\psi} &= \frac{1}{N}\sum_{k=1}^{N} \psi_i(t_k)\psi_j(t_k) \\ &= \frac{1}{N}\sum_{k=1}^{N} [q_i(t_k)q_j(t_k) + \gamma q_j(t_k) + q_i(t_k)\gamma + \gamma^2]\end{aligned} \tag{7}$$

For practical systems having low to moderate damping and finite sample size, it can be understood from equation 7 that POC provides a good approximation to the true linear modal component which deviates from each other as damping increases. Hence the POC covariance matrix $\mathbf{R_\Psi}$ is still expected to show a diagonally dominant behavior in the limit as $N \to \infty$ and when the errors are low (i.e., low to moderate damping) ([41, 42]).

The main objective of RPCA is to provide a recursive estimate of $\mathbf{W}$ as well as $\psi_k$ at each time instant as and when the data streams in real time. For structural systems with low to moderate damping, obtaining the POCs at each time instant is equivalent to obtaining the normal coordinates at each instant. Since the normal coordinates are independent, they are likely to be mono-component in nature, thereby a lower order time series model would be sufficient to capture the dynamics of the same.

The response covariance matrix $\mathbf{R_k}$ at any instant $k$ can be written as a function of the covariance matrix of the of the previous time instant $\mathbf{R}_{k-1}$ and response vector $\mathbf{x_k}$ at the $k^{th}$ time instant as shown:

$$\mathbf{R}_k = \frac{k-1}{k}\mathbf{R}_{k-1} + \frac{1}{k}\mathbf{x}_k\mathbf{x}_k^T \tag{8}$$

The covariance estimate $R_k$ can we written in terms of its eigen value decomposition as $[\mathbf{R}_k] = [\mathbf{W}_k]\,[\mathbf{\Upsilon}_k]\,[\mathbf{W}_k]^T$.

On substituting in equation(8), the expression for the covariance matrix is rewritten as

$$\mathbf{W}_k \boldsymbol{\Upsilon}_k \mathbf{W}_k^T = \frac{k-1}{k} \mathbf{W}_{k-1} \boldsymbol{\Upsilon}_{k-1} \mathbf{W}_{k-1}^T + \frac{1}{k} \mathbf{x}_k \mathbf{x}_k^T \tag{9}$$

The estimate POC vector at $k^{th}$ time instant can be written as $\left\{\tilde{\psi}_k\right\} = [\mathbf{W}_{k-1}]^T \{\mathbf{x}_k\}$. On substituting in equation(9), the following expression can be obtained

$$[\mathbf{W}_k]\,[k\boldsymbol{\Upsilon}_k]\,[\mathbf{W}_k]^T = \mathbf{W}_{k-1}\left[(k-1)\,\boldsymbol{\Upsilon}_{k-1} + \tilde{\psi}_k \tilde{\psi}_k^T\right] \mathbf{W}_{k-1}^T \tag{10}$$

For the RPCA algorithm to be stable and robust, it is important that the term $[(k-1)\,\boldsymbol{\Upsilon}_{k-1} + \tilde{\psi}_k \tilde{\psi}_k^T]$ is diagonally dominant, in order to evaluate the EVD by using Gershgorin's theorem ([43]). The term $\tilde{\psi}_k \tilde{\psi}_k^T$ represents the correlation between the POC estimates at a particular instant. Substituting from equation 6, the covariance between POC estimates can be written as (to an arbitrary scale factor):

$$\begin{aligned} \tilde{\psi}_k \tilde{\psi}_k^T &= \mathbf{W}_{k-1}^T x_k {x_k}^T \mathbf{W}_{k-1} \\ &= (q_{k-1} + \gamma)({q_{k-1}}^T + \gamma^T) \\ &= q_{k-1} {q_{k-1}}^T + \gamma {q_{k-1}}^T + \gamma^T q_{k-1} + \gamma \gamma^T \end{aligned} \tag{11}$$

As far as the dynamics of structural systems are considered, the error term in the equation 11 can be neglected as the number of sampling points increases and under moderate to low damping ([41, 42]). The first term in equation 11 resembles the covariance of the normal coordinates at the instant $(k-1)$, which are in turn mono-component in nature. Thus the term $q_{k-1} {q_{k-1}}^T$ represents a matrix whose diagonal terms dominate its off-diagonal terms; hence, the term $\tilde{\psi}_k \tilde{\psi}_k^T$ can be safely assumed to be diagonally dominant. This in turn, ensures the diagonal dominance of the matrix $\left[(k-1)\Upsilon_{k-1} + \tilde{\psi}_k \tilde{\psi}_k^T\right]$, facilitating straightforward application of Gershgorin's theorem. For first order dynamical systems such as chemical systems ([15]), the above equations would not hold true automatically and the concept of diagonal dominance has to be enforced upon, for the application of Gershgorin's theorem. Hence for a structural system, the recursive eigen space update is obtained using a first order perturbation (FOP) approach which provides a less computationally intensive algorithm in a recursive framework. The EVD of the matrix $\left[(k-1)\Upsilon_{k-1} + \tilde{\psi}_k \tilde{\psi}_k^T\right]$ can be substituted as $\mathrm{H_k} \boldsymbol{\Lambda}_k \mathbf{H}_k^T$ into equation(9) as,

$$[\mathbf{W}_k][k\boldsymbol{\Upsilon}_k][\mathbf{W}_k]^T = [\mathbf{W}_{k-1}\mathbf{H}_k][\boldsymbol{\Lambda}_k][\mathbf{W}_{k-1}\mathbf{H}_k]^T \tag{12}$$

which yields the following iterative update equations:

$$\left.\begin{aligned} \mathbf{W}_k &= \mathbf{W}_{k-1}\mathrm{H}_k \\ \Upsilon_k &= \frac{\Lambda_k}{k} \end{aligned}\right\} \tag{13}$$

The recursive algorithm of equation(8) is transformed to obtain the values of $H_k$ and $\Lambda_k$. Since the term $(k-1)\,\Upsilon_{k-1} + \tilde{\psi}_k\tilde{\psi}_k^T$ is diagonally dominant, the eigen values can be assumed to be the diagonal entries of the matrix. Hence the $i^{th}$ diagonal entry of the term $\Lambda_k$ can be represented as $(k-1)\,\lambda_i + \tilde{\psi}_i^2$, where $\lambda_i$ is the $(i,i)$ element of $\Upsilon_{k-1}$ and $\psi_i$ is the $i^{th}$ entry of the POC estimate. Once the eigen values are known, the corresponding eigen vectors can be found out, leading to $H_k$.

One of the key problems faced while applying FOP approach is that the recursive eigen vectors obtained at each time instant are not ordered, which poses the problem of permutation ambiguity([24, 44]). This can be addressed by arranging the basis vectors according to decreasing order of the corresponding eigenvalues in $\Upsilon_k$. At each time instant, the eigenvalues indicate the contribution of the particular eigenvectors. The contribution factor can for a particular $i^{th}$ eigen vector $w_i$ at each time instant can be written as $\frac{\alpha_i^2}{\sum_{i=1}^{n}\alpha_i^2}$, where $\alpha_i^2$ is the eigenvalue corresponding to $w_i$. Let $\mathbf{W}_k = [\mathbf{W}_k^1\mathbf{W}_k^2]$, where $\mathbf{W}_k^1$ is the subspace at $k^{th}$ time instant consisting of eigenvectors, that account for more than 90% of the energy in the participating modes of the system. These recursively estimated subspaces, are the subsequently utilized to find the true POC at each instant of time as per the expression

$$\psi_k = \mathbf{W}_k^T\mathbf{x}_k. \tag{14}$$

The first element of the $\psi_k$ vector represents the major principal component. TVAR modeling is now performed on the first major principal component.

### *2.2. **TVAR modeling***

The RPCA algorithm provides the POC updates recursively at each instant of time. Once the modal responses are obtained using the proposed algorithm, the next step is to find out the instant of damage. In order to characterize the behavior of the POC updates(which can be approximated to normal coordinates), TVAR modeling is adopted here ([14]). The use of TVAR modeling for detecting structural damages has been attempted in the

recent times with fair amount of success([10]). TVAR coefficients of the modeled transformed response are tracked in real time in order to identify the damage instant. The sudden changes in AR coefficients indicate the alterations in the dynamical properties of the system, such as shifts in natural frequencies, changes in the mode shapes of the system, etc., induced due to the damage occurred in the system. In the proposed work, the transformed response (i.e.,the first POC) extracted from the RPCA algorithm is modeled using a TVAR model. However, the main drawback associated with using TVAR models is the selection of model order a priori such that the resulting TVAR model correctly characterizes the data during the times of interest. The use of POCs instead of the raw vibration data, whose near resemblance to normal coordinates enables the use of a low model order, resolves the issue of model order selection.

Let $\psi^1(k)$ represent the POC at any instant which captures the maximum kinetic energy of the system and let $v(k)$ denote the zero mean Gaussian white noise with variance $\sigma_v^2$. Then the AR model of order p can be represented as:

$$\psi^1(k) = \sum_{i=1}^{p} a_i \psi^1(k-i) + v(k) \tag{15}$$

The non stationary nature of the POC, necessitates recursive updates of the AR coefficients in which $a_i$ becomes $a_i(t)$, to capture the dynamics of the normal coordinate effectively. For this purpose, the Kalman filter is utilized to estimate these time-varying coefficients, knowing the observations of data ([14]). The following equation is the discrete representation of the $a_i(t)$ coefficients and $w(k)$ is the process noise with variance $\sigma_w^2$ and covariance, $\mathbf{P_w} = \mathbf{I_{p\times p}}\sigma_\mathbf{w}^\mathbf{2}$. Both noise measurements $v(k)$ and $w(k)$ are mutually independent and uncorrelated. Consider the following set of equations, where the unknown state vector $b(k)$ is expressed as shown:

$$\begin{aligned} \mathbf{b(k)} &= \mathbf{\Gamma(k-1)b(k-1)} + \mathbf{w(k)} \\ \boldsymbol{\psi}^\mathbf{1}\mathbf{(k)} &= \mathbf{C(k)b(k)} + \mathbf{v(k)} \end{aligned} \tag{16}$$

The state vector $b(k)$ is given by: $\mathbf{b}(k) = \left[a_1(k), a_2(k), \ldots\ldots a_p(k)\right]^T$. The matrix $\mathbf{\Gamma}(k-1)$ is an identity matrix ($\mathbf{I}_{p\times p}$). The matrix $C_k$ is the observation data with discrete $k$ steps given as: $\mathbf{C}(k) = \left[\psi^1(k-1), \psi^1(k-2)\ldots\ldots\psi^1(k-p)\right]$. The Kalman filter has mainly two processes: one is the stepwise time update (prediction) and the other one is measurement update (correction) of the predicted data. At each step, the set of the Kalman filter equations can

be written as ([3, 14]):

$$\begin{aligned}
\mathbf{b}\left(k|k-1\right) &= \mathbf{b}\left(k-1|k-1\right) \\
\mathbf{P}_b\left(k|k-1\right) &= \mathbf{P}_b\left(k-1|k-1\right) + \mathbf{I}\sigma_w^2 \\
\psi^1\left(k|k-1\right) &= \mathbf{C}\left(k\right)\mathbf{b}\left(k|k-1\right) \\
\sigma_{\psi^1}^2\left(k|k-1\right) &= \mathbf{C}\left(k\right)\mathbf{P}_b\left(k|k-1\right)\mathbf{C}(k)^T + \sigma_v^2
\end{aligned} \tag{17}$$

And,

$$\begin{aligned}
\mathbf{KG}\left(k\right) &= \mathbf{P}_b\left(k|k-1\right)\mathbf{C}(k)^T\sigma_{\psi^1}^2(k|k-1)^{-1} \\
\mathbf{b}\left(k|k\right) &= \mathbf{b}\left(k|k-1\right) - \mathbf{KG}\left(k\right)\left[\psi^1\left(k\right) - \psi^1\left(k|k-1\right)\right] \\
\mathbf{P}_b(k|k) &= [\mathbf{I} - \mathbf{KG}(k)\mathbf{C}(k)]\mathbf{P}_b(k|k-1)]
\end{aligned} \tag{18}$$

where $\mathbf{b}\left(k|k-1\right)$ represents a priori estimate and its linear combination would result in $\mathbf{b}\left(k|k\right)$, which is a posteriori. The Kalman gain $KG(k)$ gives a weightage to the prediction error $\psi^1\left(k\right) - \psi^1\left(k|k-1\right)$, to minimize the state estimation error $\mathbf{b}\left(k|k\right)$. The apriori and the posteriori covariance estimates are given by $\mathbf{P}_b\left(k|k-1\right)$ and $\mathbf{P}_b\left(k|k-1\right)$, respectively. Although the TVAR model facilitates adequate representation of the non stationary transformed response, but in order to use it for damage detection, only TVAR model is not enough; hence, DSF are applied on the TVAR coefficients to detect damage as described next. Alongside TVAR coefficients, these statistical indicators (or the DSF) are applied to detect damage which run in real time. These DSF have a real time fervor and hence, these are amenable towards online implementation and has been explored in the present context.

## 3. Damage Sensitive Features

In the present framework, RPCA facilitates online processing of data producing recursive updates of eigen vectors and eigen values, referred to as eigen subspace. The eigen subspace by themselves cannot detect the change in system properties inflicted due to damage, if not processed by a set of damage markers commonly referred to as damage sensitive features (DSF) ([1, 37, 45]). The primary requirements of good damage sensitive features are their ability to detect the presence of damage, effectively distinguish between the damaged and undamaged states of the structure, followed by their capacity to possibly locate and quantify the extent of damage. Additionally, to detect damages in real time, the proposed DSFs should be amenable for online

implementation and should accurately identify the presence of damage as and when the response data streams in continuously. Several damage detection and SHM techniques have been proposed in the literature ([4, 5, 6]) that involve use of specific DSFs whose changes signify damage to the system. Examples of DSF used in SHM literature for damage detection include finite difference approximation on mode shapes ([46]), localization indices (LI1 and LI2) based on auto regressive (AR) coefficients ([36]), various strain related parameters, global integrity index based on shifts in natural frequency ([15]), curvature mode shape technique ([47]), etc.

The disadvantages associated with the traditional DSFs includes requirement of (**i**) baseline or reference data from a healthy structure; (**ii**) windowing of response data etc., which impedes their application in an online framework. In this section, a brief background on the formulation of *online DSFs* is proposed utilizing the concepts of TVAR coefficients and recursive signal statistics. These features are based on the reorientation of eigenspace due to damage which is manifested in the form of change in the pattern of TVAR modeling before and after damage. In the following sections, TVAR coefficients ($a_i$), signal statistics on AR coefficients ($\mu_{a_i}$,$\zeta_{a_i}$), spatial recursive residual errors ($\varepsilon_{RR}$) are presented.

### *3.1. **Time varying auto-regressive coefficients***

The key DSF utilized in the paper is the TVAR coefficients. The motivation for this DSF is derived from the use of AR coefficients as a criterion for novelty evaluation ([48]), which presents the use of a statistical parameter known as Mahalanobis distance value, for AR coefficients to distinguish between a damaged state and an undamaged state. However, this parameter frequently requires the use of windowing and baseline data to detect damage, thus it is not possible to implement it in an online framework. These drawbacks of traditional AR modeling motivates the development of TVAR modeling ([14]) which provides a recursive update of AR coefficients in real-time, enabling it to capture the non stationary nature associated the data due to damage. The near mono-component nature of the transformed response ensures that low model order is sufficient to capture its dynamics; therefore, in the proposed framework, a model order of 2 (two) is pre-selected for all the cases. The basic equation 15 becomes:

$$\psi^1(k) = a_1(k)\psi^1(k-1) + a_2(k)\psi^1(k-2) + v(k) \tag{19}$$

where the symbols carry the same meaning as that of equation 15. Although $a_1$ and $a_2$ are expected to alter mildly at each time instants, the damage instant is characterized by sudden changes in the overall behavior of TVAR coefficients post damage. Tracking this change in $a_1$ and $a_2$ serve as an indicator of damage.

### *3.2. **Recursive statistics on TVAR coefficients***

The AR coefficients extracted from the TVAR modeling on the transformed response is discussed in detail later to show modulatory/wavy behaviors, which can mask the accurate determination of damage instant. This is partly attributed to the non stationarity nature of the transformed response ($\psi(t)$) and also due to transformed response not being purely mono-component. As explained in Section 2.1, the POC tends to normal coordinates only under certain assumptions which may not be realized in practise always. Hence, even though TVAR coefficients reflect the damage in a system, the change may not be always obvious. To address the aforementioned issue, recursive versions of the commonly used signal statistics are employed on TVAR coefficients ([38]). The damage in a structural system is corroborated by the change in the behavior of AR coefficients which is manifested in the form of : (**i**) sharp peak in $a_1$ and/or $a_2$ in the vicinity of damage; (**ii**) drift of post damage $a_1$ and/or $a_2$ from the pre-damage values. This prompted the use of recursive mean ($\mu_{a_i}$), and higher moments ($\zeta_{a_i}$) of AR coefficients which can capture the essence of damage in a better way.

$$
\begin{aligned}
\mu_{a_i}(k) &= \frac{k-1}{k}\mu_{a_i}(k-1) + \frac{1}{k}a_i(k) \\
{\sigma^2}_{a_i}(k) &= \frac{k-1}{k}{\sigma^2}_{a_i}(k-1) + \frac{1}{k}a_i(k)a_i(k) \\
\zeta_{a_i}(k) &= \frac{(k-1)\zeta_{a_i}(k)/k + a_i(k)a_i(k)a_i(k)a_i(k)a_i(k)a_i(k)/k}{((k-1)\sigma^2_{a_i}(k-1)/k + a_i(k)a_i(k)/k)^3}
\end{aligned}
\tag{20}
$$

where $\zeta_{a_i}$ refers to the sixth moment and $\sigma^2_{a_i}$ refers to the second moment or variance.

### *3.3. **Temporal RRE for Local damage detection***

Addressing the facets of structural damage detection involves a close investigation of temporal and spatial damage identification which becomes difficult especially when attempted simultaneously in an online framework. In the present work, the authors have tried to investigate the aspects of spatio-temporal damage detection in

the same framework with a reasonable degree of accuracy. To address damage localization, the term recursive residual error (also known as local RRE) is defined and expressed for each degree of freedom ($\varepsilon_{RR}$). However, a stringent assumption involved for this framework is that when a column of a multi degree of freedom (mdof) structure is damaged, its effect will be pronounced in the neighboring dofs, which in turn is manifested as a change in the RREs for that particular dof. The main motivation behind the use of residual error for damage detection has been obtained from Hot et al.([30]), which presents the use of residual error as a measure of distortion of subspaces of a nonlinear system with increase in levels of excitation.

Considering a damage at the end of $(k-1)^{th}$ instant, the subspace spanned by the updated eigenvector $\mathbf{W_k^1}$ deviates in comparison to the subspace spanned by eigen vectors at the previous time stamp $\mathbf{W_{k-1}^1}$. Apart from the instances of damage, or, the initial few seconds, it can be assumed that $\mathbf{W_k^1} \cong \mathbf{W_{k-1}^1}$, since there is no deviation in the eigenspace otherwise. Based on this assumption, the RREs due to projection of the response at a particular time instant $k$ onto $\mathbf{W_{k-1}^1}$ is evaluated as:

$$\mathbf{X}^*(k) = \mathbf{W}_{k-1}^1 * \mathbf{W}_k^{1^T} * \mathbf{X}(k) \tag{21}$$

From equation 21 it is clear that the projections of the transformed responses $\mathbf{X}^*(k)$ and the actual responses $\mathbf{X}(k)$ can be expressed as vectors with each individual element corresponding to a degree of freedom ($m$ : total number of DOFs) according to : $\mathbf{X}^*(k) = [x_1^*(k), x_2^*(k), \ldots\ldots, x_m^*(k)]^T$ and $\mathbf{X}(k) = [x_1(k), x_2(k), \ldots\ldots, x_m(k)]^T$ where $k$ represents the time instant at which RRE is estimated. Let each element of $\mathbf{X}^*(k)$ and $\mathbf{X}^*(k)$ be represented as $\mathbf{x_i}^*(k)$ and $\mathbf{x_i}(k)$ respectively, where (**i**) corresponds to a particular degree of freedom. This yields a time series of RRE (labelled as $\varepsilon_{RR} - Y_i$) corresponding to the response for each degree of freedom, which can be expressed as

$$\varepsilon_{RR} - Y_i = \left|\mathbf{x}_i^{*^2}(k) - \mathbf{x}_i^2(k)\right| \tag{22}$$

Another useful quantity in this connection is the average RRE for $i^{th}$ response for $K$ datapoints, which can be estimated according to,

$$\langle \varepsilon_{RR} - Y_i \rangle = \frac{\sum_{k=1}^{K} \left|\mathbf{x}_i^{*^2}(k) - \mathbf{x}_i^2(k)\right|}{K} \tag{23}$$

The local RRE averaged over $K$ samples is shown above. This is particularly useful, as shown later, in quantifying the percentage change in RRE (an indirect measure of loss of stiffness) before and after damage.

## 4. Proposed Algorithm

The overall methodology followed in the paper entails the amalgamation of separate modules which detect two key ingredients: temporal and spatial damage detection, simultaneously. The first module deals with the temporal damage detection, wherein the raw acceleration data is processed by the RPCA algorithm as the data streams in real time. This accounts for an online damage detection framework as no batches of data are utilized in order to form a baseline. TVAR modeling is done on the updated first principal component which yields TVAR coefficients at each instant of time. As previously explained, TVAR coefficients are tracked online for any major and minor changes. Damage sensitive feature (like higher moments) are utilized to corroborate the instant of damage, when it cannot be discerned directly by tracking TVAR coefficients only. Once the damage instant is detected, the spatial damage detection module further resolves the location of damage. The basic steps of the algorithm is enumerated as follows:

The basic steps of the algorithm are enumerated as follows:

1. First, batch PCA is employed on some initial data points in order to estimate the initial eigen vector and eigen value matrices.
2. The RPCA algorithm then operates online on the real time input of the streaming data.
3. Using the recursive gain depth parameter, the covariance estimate at the present time instant is derived using the covariance estimate at preceding time instant. From the recursive updates, the eigen vector and eigen value matrices are updated using FOP approach and the transformed responses (principal components) are obtained using the RPCA algorithm.
4. The proposed time series models are generated based on the responses and a TVAR model is fit. The DSF are tracked realtime in order to extract the changes in the model coefficients, thereby revealing the faults in the system.
5. Once the instant of damage is determined, the algorithm shifts on to the next module where the spatial detection of damage takes place. The local RREs are tracked online recursively to capture the spatial effect of the damage, visually.

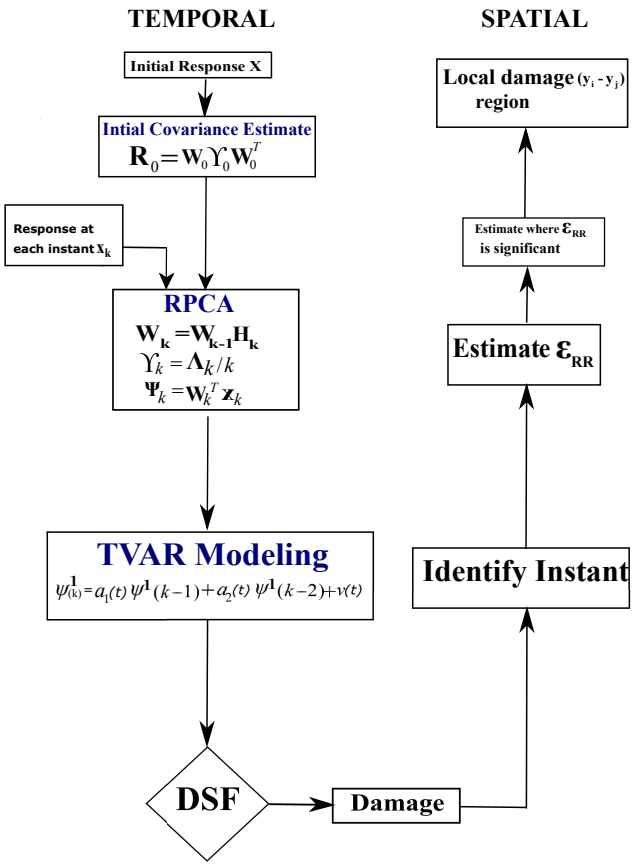


Figure 1: Flow chart of the proposed algorithm

A flowchart as shown in Figure 1 outlines the proposed damage detection scheme, stepwise. Vibration responses are processed by the RPCA algorithm to obtain the transformed responses, then the TVAR modeling is utilized to extract the time-varying coefficients through which damage instant is detected. It is to be noted that the aforementioned proposed algorithm has the following few characteristics: (**i**) the data is processed at each time instant, as and when it becomes available, i.e the algorithm works online. (**ii**) to locate the instant of damage a reference value (baseline) is not required, i.e. it is baseline free. (**iii**) there are no parameters controlling the working of the algorithm, hence its parameter free. The above mentioned characteristics of the proposed algorithm makes it an ideal choice for a real time damage detection framework.

## 5. Numerical Example

In order to illustrate an application of the proposed method, numerical simulations are carried out on a 5-storey model having a buoc-wen oscillator at its base degree of freedom to simulate a nonlinear change of state which is defined as damage. The level of nonlinearity is controlled by the parameter $\kappa$, which is used to scale the nonlinear force term. Two kinds of excitations are used: stationary zero mean Gaussian white noise for a duration of 50$s$ and an earthquake excitation (El Centro ground motion). The excitation are sampled at 50 Hz. Towards this simulation example, the model is described first followed by the analysis of the results.

### *5.1. Model Description*

TThe model under study is similar to the one as presented by Ramallo et al. ([49]). Numerical simulations are carried out on the model which consists of 4 floors and a base which is separated from the surrounding soil by an LRB base isolator. Upon subjecting the system to an external excitation vector $\mathbf{u}$, the state equations for this system can be written as:

$$\begin{aligned} \dot{\mathbf{x}} &= \mathbf{A}\mathbf{x} + \mathbf{E}\mathbf{u} \\ \mathbf{y} &= \mathbf{B}\mathbf{x} \end{aligned} \tag{24}$$

Here, the vector $\mathbf{x}$ is the vector of states and the vector $\mathbf{y}$ represents the output vector, which is governed by the $\mathbf{B}$ matrix. The inherent properties of the system , i.e., the system matrix, $\mathbf{A}$, and the excitation matrix $\mathbf{E}$ are given by

$$\begin{aligned} \mathbf{A} &= \begin{bmatrix} [\mathbf{O}]_{5\times5} & [\mathbf{I}]_{5\times5} \\ -\mathbf{M}^{-1}\mathbf{K} & -\mathbf{M}^{-1}\mathbf{C} \end{bmatrix} \\ \mathbf{E} &= \begin{bmatrix} 0 & 0 & 0 & 0 & 0 & -\frac{1}{m} & -\frac{1}{m} & -\frac{1}{m} & -\frac{1}{m} & -\frac{1}{m} \end{bmatrix}^T \end{aligned} \tag{25}$$

The equation of motion for the system can be summarized as:

$$\mathbf{M}\ddot{x} + \mathbf{C}\dot{x} + \mathbf{K}x = \mathbf{\Lambda}f - \mathbf{M}\mathbf{I}\ddot{\mathbf{x}}_\mathbf{g} \tag{26}$$

where, $\mathbf{M}$, $\mathbf{C}$, and $\mathbf{K}$ are the assembled mass, damping, and stiffness matrices, respectively. A simple shear building representation is assumed to arrive at the expressions for $\mathbf{M}$, $\mathbf{C}$, and $\mathbf{K}$ which are skipped here for

brevity. The mass at each of the four floor levels from the top is 7461 kg and at the base is 6800 kg. The damping coefficients for each floor level above the base is 23.71 kNs/m and 3.74 kNs/m for the base. The stiffness coefficients for each of the floors above the base is 11912kN/m and that for the base is 232 kN/m.

The parameter $\mathbf{\Lambda}$ in equation(26) represents the location of the base at the point of application of the force due to the LRB base isolator and $\ddot{\mathbf{x}}_\mathbf{g}$ represents the ground acceleration. The forces due to base damping and stiffness terms ($k_b$ and $c_b$) have been included in the non-linear force term ($f$) due to the LRB base isolator, which can be expressed as:

$$f = \kappa z Q_{pb} - k_b x_b - c_b \dot{x}_b \tag{27}$$

where, $Q_{pb} = \left(1 - \frac{k_{yield}}{k_{initial}}\right)$ and $k_b$ and $c_b$ are the stiffness and the viscous damping respectively, in the horizontal direction. The initial and the post yield shear stiffness are given by $k_{initial}$ and $k_{yield}$, respectively. The evolutionary variable $z$ is used to provide the hysteretic component of the horizontal force, $Q_{hyst} = zQ_{pb}$. The variable $z$ can be obtained by solving the following nonlinear differential equation:

$$z = -\gamma z \left|\dot{x}_b\right| \left|z^{n-1}\right| - \beta \dot{x}_b \left|z^n\right| + A\dot{x}_b \tag{28}$$

where $\gamma, \beta, A$ and $n$ are the shape parameters of the hysteresis loop. ([49]) . For the current model, $A = \left(\frac{k_{yield}}{k_{initial}}\right)$, $\gamma = \beta$ and $n$=1. The yield force $Q_y$ is selected as 5% of the total weight of the building which gives $Q_y$ = 17800 kg and pre-yield to post- yield stiffness ratio $\left(\frac{k_{yield}}{k_{initial}}\right) = 6$. For the present study of the model, the values of the parameters are set as: $\gamma$=$\beta$=39.1. The constant $\kappa$ has been introduced in equation 27 to control the nonlinear force term. For the purpose of inducing a damage, the authors have proposed to vary the value of $\kappa$ in the equation of motion. For instance, a change in $\kappa$ from 1 to 0.7 is conveniently assumed as a 30% change in nonlinear characteristics of the system.

### *5.2.* ***Results for White Noise***

The system is subjected to Gaussian white noise excitation as described in the previous section. The algorithm starts off with an initial covariance estimate and slowly progresses as outlined in Section (4). Temporal damage detection cases are studied first by sequentially changing the $\kappa$ corresponding to 15%, 25%, 40% and 50% changes in nonlinear characteristics respectively. Once the temporal damage detection is carried out, the

examples for spatial detection are described next.

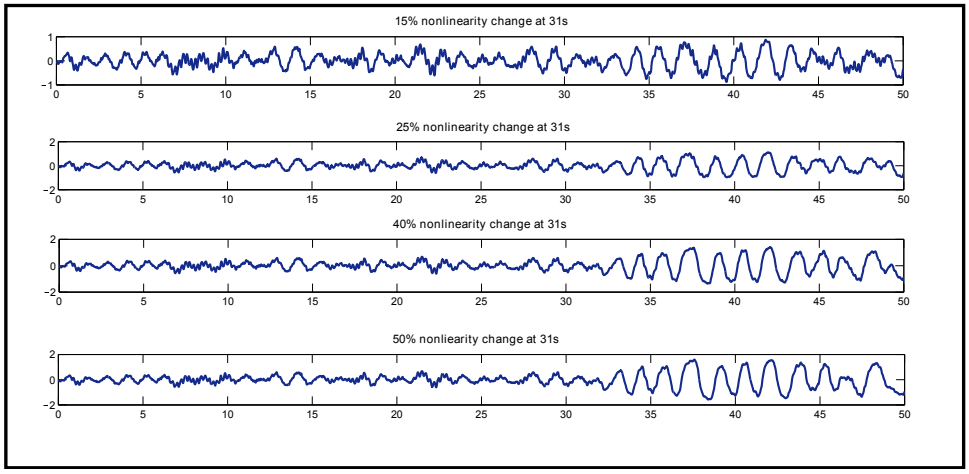


Figure 2: Acceleration plots for white noise excitation for different cases of non linearity

### *5.2.1. **Temporal damage detection results***

The response of the top floor of the 5 dof model has been shown in Figure 2. The damage is induced through change of nonlinearity by 15%, 20%, 40% and 50% at a particular time instant of 31s. As evident from the figure, the changes due to 15%, 20%, 40% cannot be directly discerned from the response data, visually. In order to detect the temporal damage, two DSFs are used- TVAR coefficients, Recursive Mean of AR coefficients . It can be clearly observed from Figure 3 that the damage instant can be easily detected using the AR coefficients by exploiting their sudden changes at the damage instant. Thus, it confirms that TVAR modeling is amenable to online damage detection in a recursive framework. It should be noted that selection of model order for a time series needs a fair amount of mathematical insight into the observations. Since the transformed responses obtained using the RPCA algorithm are mono-component in nature, a relatively low model order (say,2) can be used, which is shown in Figure 3. It can also be observed from Figure 3(b) that recursive mean could capture the essence of fault detection where it shows a significant deviation in its original trajectory at 31$s$. However, it will be shown in the following sections that the plots for higher order moments provide much accurate results than recursive mean as observed for El Centro excitation and practical implementation cases.

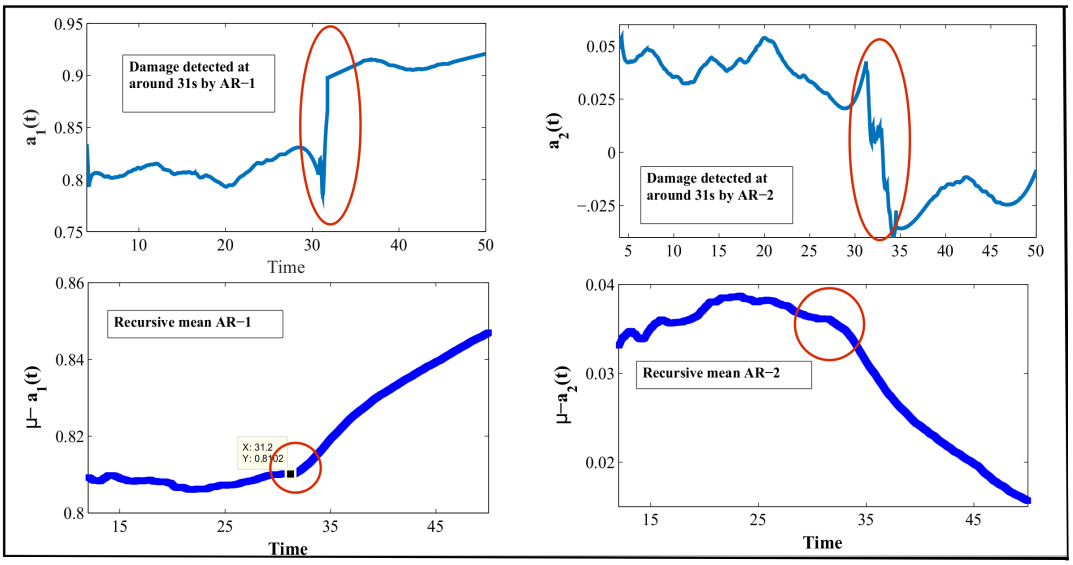


Figure 3: Damage detection using damage sensitive features for 30% non linearity change

The efficacy of recursive DSF is less effective for lower percentage change in nonlinearity. As evident from literature, damages of the order of 25% have been often reported as a lower limit for vibration based damage detection ([10, 23]). However, in the present work the use of TVAR coefficients successfully detects damage corresponding to 15% change in nonlinearity. As seen from Figure 4, the TVAR plots serve as a robust DSF for detecting damage. The damage instant can be clearly identified from the figure as 31$s$ using the proposed method.

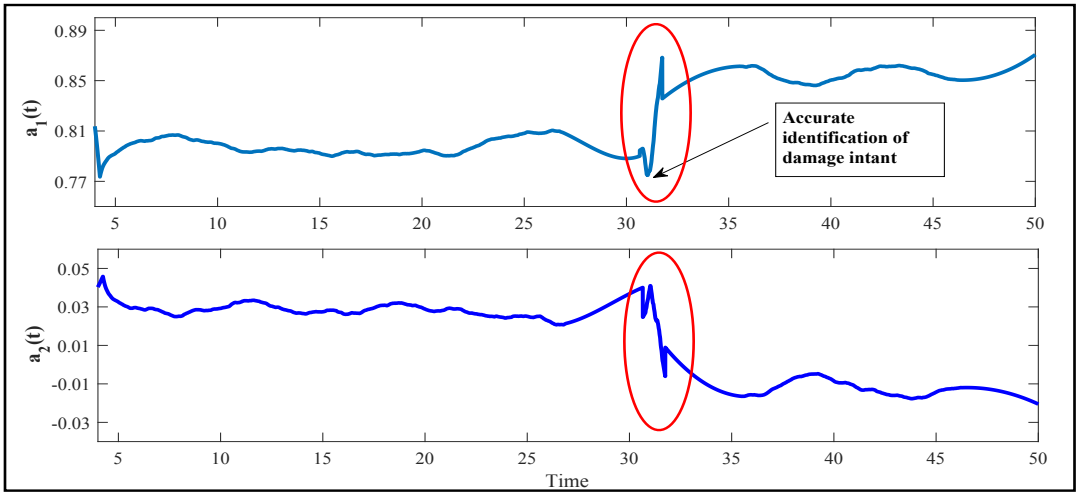


Figure 4: Damage detection using AR coefficients for 15% non linearity change

In order to further validate the damage instant, the authors have proposed the use of recursive mean on the TVAR coefficients which are tracked to show any significant changes, online. By looking at figures 5(a) and 5(b), it can be seen that there is a significant change in the estimate of the recursive mean. It can also be observed from the figures that the DSF utilized for tracking the changes shows distinct peaks indicating the exact instant of damage occurred in the system.

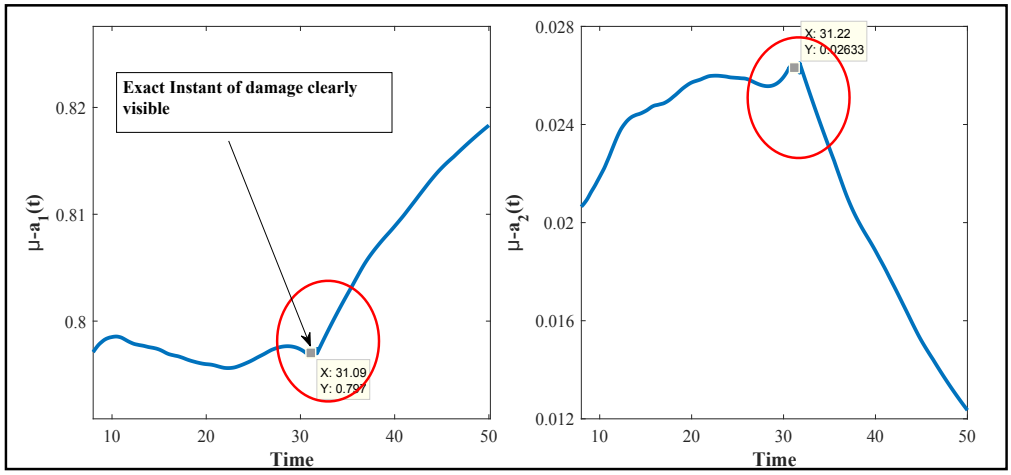


Figure 5: Damage detection using recursive mean for 15% non linearity change

### 5.3. *Spatial Damage Detection Results*

In the previous sections, the concept of global damage has been discussed which was introduced by varying the nonlinear force term $\kappa$ in the equation of motion of the system. In the present section, the notion of local damage is presented by a change in stiffness for a particular floor which brings out the concept of online spatio-temporal damage detection. As already mentioned, only when the instant of damage in ascertained, the algorithm shifts on to spatial damage detection module in order to find out the location of the damage. The simultaneous temporal and spatial case deals with 35% and 25% changes in linear stiffness in the $3^{rd}$ storey of the structure. The system is assumed to be fully nonlinear by scaling the value $\kappa$ to 1. Once the damage instant is detected by tracking the change in AR coefficients, the spatial module starts functioning online in order to localize the position of damage occurred in the system. From Figure 6, it can be shown that clear damage instant is identified at 31s for a 35% damage. Once the damage instant is detected, the spatial RRE in

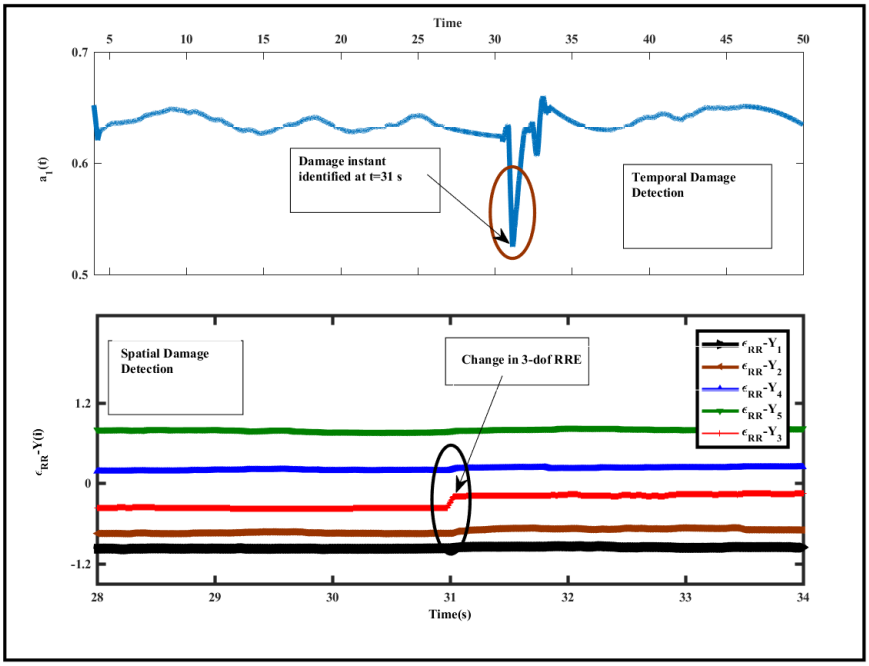


Figure 6: Comparison between spatial and temporal damage for 35% change

the neighborhood of the vicinity of damage (say, 29s to 33s) is examined. From the same figure, it is clearly observed that the spatial RRE for third degree of freedom shows a significant change at 31s compared to the other set of responses which indicates that the damage has occurred in the third storey. From Figure 7, it is evident that the the spatial RRE for 25% damage indicates a visible change at t=31s. As outlined before, the temporal and spatial detection module should run simultaneously. The changes in the TVAR coefficients and the local RRE are tracked online recursively in order to capture the essence of temporal and spatial damage detection, respectively. As seen from Figures 6 and 7, damage detection can be interpreted from the change in local RRE corresponding to the third dof which substantiates the localization of the damage. However, as the extent of stiffness degradation decreases, detecting spatial damage becomes increasingly difficult as compared to detecting temporal damage alone as evident from Figure 7.

### *5.4. **Results for Elcentro ground excitation***

To illustrate the potential application of the proposed method, numerical simulation is performed on the 5 dof buocwen model using El Centro excitation data. The damage is simulated for a 30% change at 25s. The

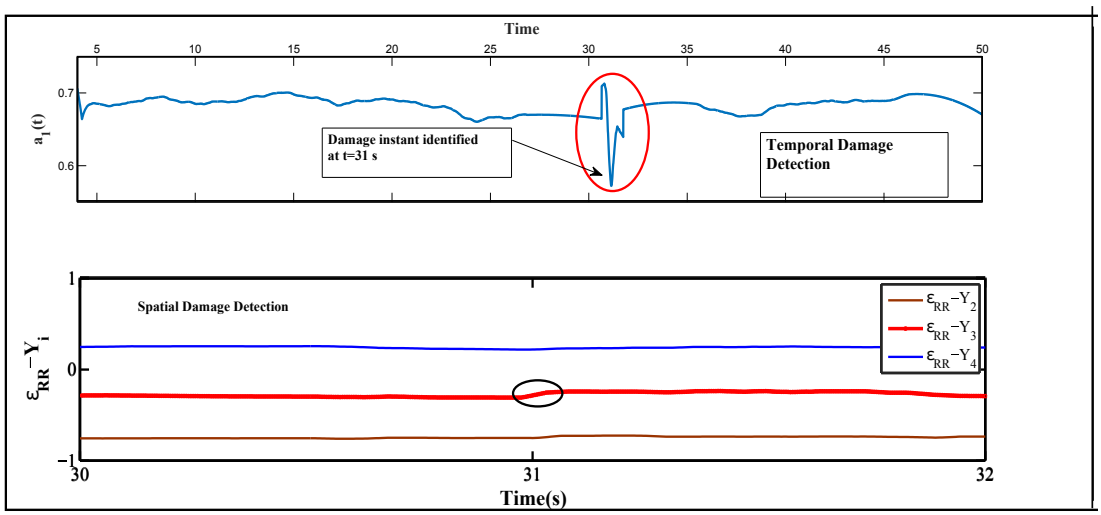


Figure 7: Comparison between spatial and temporal damage for 25% change

proposed algorithm processes the data and the simultaneous tracking of the DSF are done online, recursively, in order to accurately identify the damage instant. From Figure 8, it can be seen that the plots of TVAR coefficients do not indicate a clear instant of damage due to the highly non-stationary behavior of the input excitation. In order to mask the non-stationary behavior of the input data, the authors have proposed the use of higher order moments (HOM) of the TVAR coefficients to clearly indicate the instant of damage. The effect of damage on HOM is much more significant than the effect of local non-stationarity associated with the input excitation, thereby making the HOM such as the sixth moment($\zeta_{a_i}$) better equipped to capture the essence of damage. In the present damage scenario, the sixth moment of the TVAR coefficients($\zeta_{a_1}(t)$,$\zeta_{a_2}(t)$) are effectively used to indicate the instant of damage by observing a change in the level of the plots. As observed from Figure 8, plots for sixth order cumulant for $a_1(t)$ and $a_2(t)$ show sudden change in the level of the graph. While approaching the damage instant, the plots show a significant change in the level which validates that the damage has indeed occurred at t=25s. It should however be noted that simultaneous spatial and temporal damage detection is difficult in this case owing to amplitude non-stationarity of the ground motion.

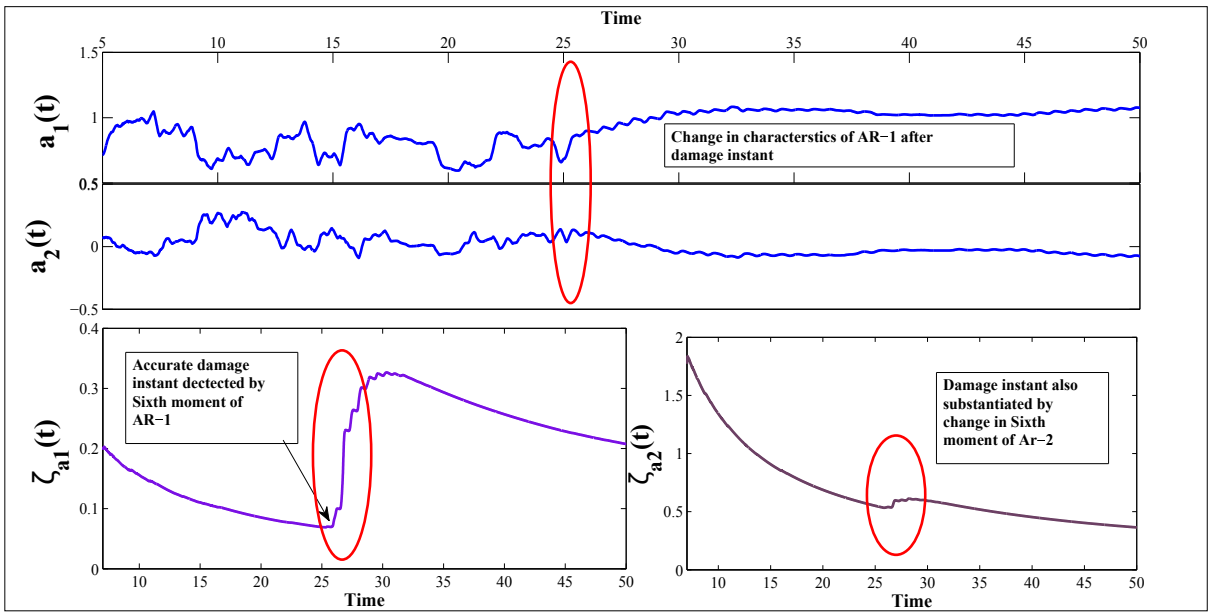


Figure 8: DSF for El Centro excitation for 30% change

### *5.4.1.* ***Comparative study with batch PCA***

In this section, a comparison is made between the performance of basic PCA with the RPCA. The 5 dof bouc-wen model described in section 5.1 is excited using the El Centro ground motion and and 30% change in nonlinearity was introduced in the system at $t = 25s$. The transformed responses obtained from the RPCA and the traditional batch PCA algorithms are utilized to fit in individual TVAR models. Recursive HOM employed on the TVAR coefficients revealed the subtle differences between the algorithms which is depicted in Figure 9. While the RPCA algorithm processes the data at each time instant and provides eigen space updates in real-time which are subsequently utilized to model the transformed response using TVAR parameters, batch PCA works by accumulating the data into $10s$ windows and provides eigen space at the end of each window size. This eigen space is assumed to be constant over the entire interval and transformed response for the a particular window $w_i$, is obtained using the equation

$$\psi^{w_i} = \mathbf{W}^{w_i T}\mathbf{X}^{w_i} \tag{29}$$

where, $\mathbf{W}^{w_i}$ is the principal orthogonal matrix or eigen vector obtained as a result of batch PCA on the response data matrix $\mathbf{X}^{w_i}$ accumulated over the corresponding window $w_i$. The initial window size is kept smaller than

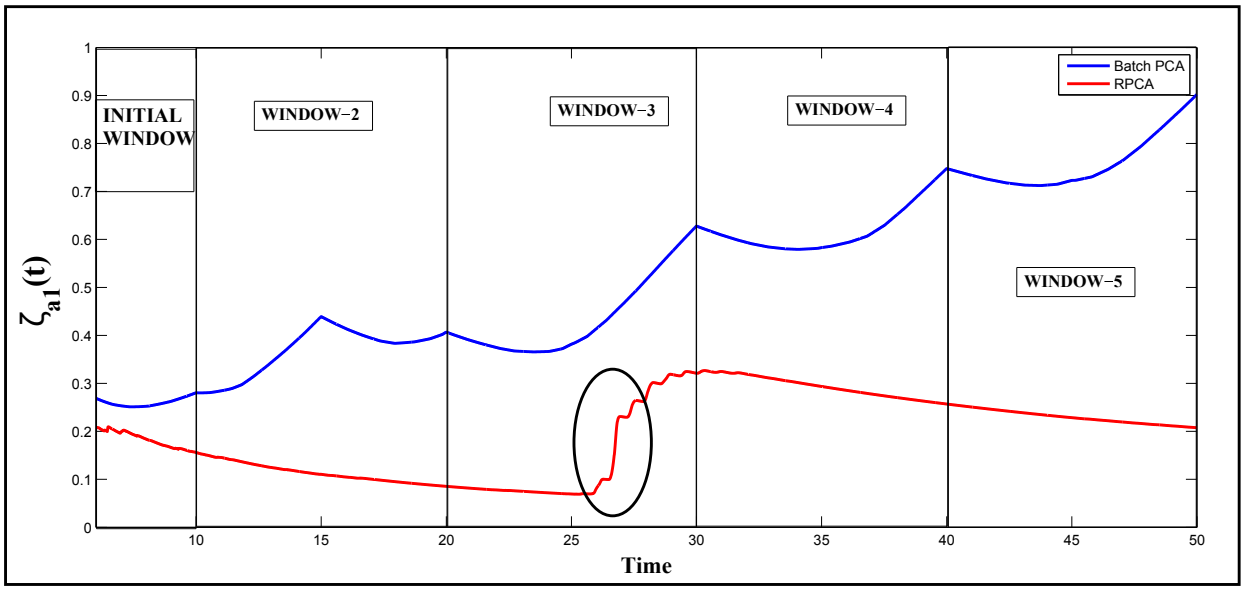


Figure 9: Comparison between batch PCA and RPCA

the rest as the batch PCA algorithm requires certain data points to stabilize. Figure 9 shows that the proposed framework using RPCA and TVAR detects the damage accurately at around 25$s$ by showing of a sharp change in the level of the $\zeta_{a_i}$ post damage. However, the algorithm using batch PCA and TVAR fails to detect the damage owing to inaccurate transformed response obtained at each window. It is clear from the figure that the plot of the batch PCA parameter, $\zeta_{a_i}$, shows discontinuity due to windowing since the transformed responses on which TVAR is modeled depends on the POMs obtained at the end of each window. Although the damage detection for the algorithm using batch PCA can be improved by reducing the window size but that would amount to increased computational cost and excess time consumption. Thus, the proposed algorithm using RPCA in conjunction with TVAR not only works in real-time but is also superior to batch PCA as evident from the the results in Figure 9.

### 5.4.2. ***Results for Underdetermined case-White Noise Excitation***

The results shown in the previous sections have been obtained by utilizing the response from all the dof, available as inputs to the algorithm. In this section, the authors have explored the applicability of the proposed algorithm for the cases where the number of sensors is less than the number of degrees of freedom, which is

referred to as an underdetermined case. Physically, such a system arise in flexible systems that are instrumented with a relatively smaller number of sensors because of cost and other factors. The proposed algorithm tries to address this issue by assuming the number of degrees of freedom in the structure to be equal to number of available measurements. Hence for a 5-DOF structure, if only 3 degrees of freedom are instrumented with sensors, the proposed algorithm assumes the system to be a 3-dof structure, producing corresponding eigen-vectors (POMs) and eigen-values(POVs). Since in the proposed algorithm, TVAR modeling is done on the first transformed response, detectibility is not affected for a underdetermined system. Theoretically, the number of degree of freedoms instrumented should be at least equal to number of actively participating modes. The vibration response data from the top few dofs is of foremost importance as it has the maximum effect on the first modal response. For the case of underdetermined system, the model proposed in Section 5.1 with acceleration response data missing from second floor and fourth floor are taken for analysis. Damage was induced for the following two cases i) Global damage at 31 s ii) Local damage induced in $3^{r}d$ storey at 31s.

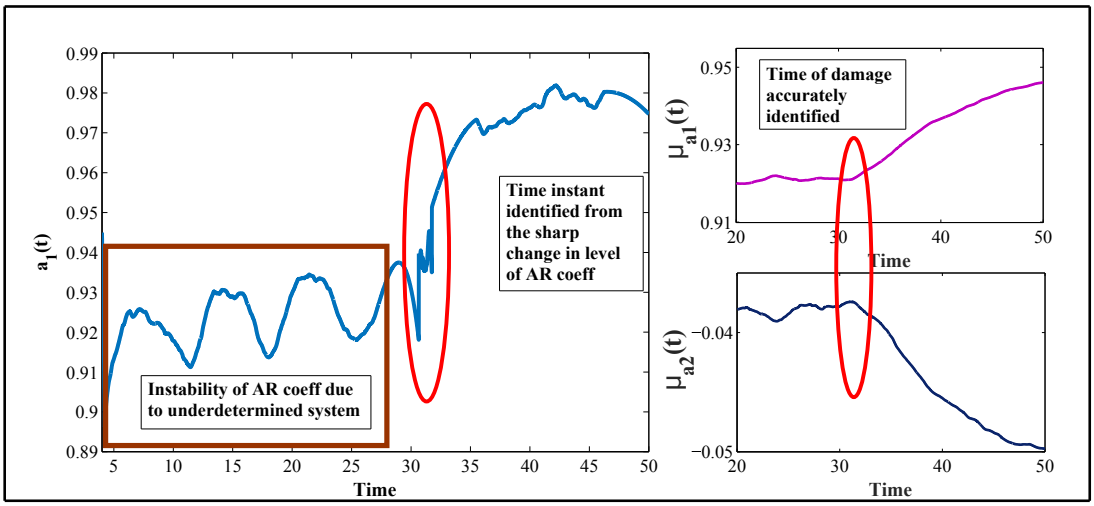


Figure 10: DSF for Underdetermined case 1- Global Damage, 20% change in nonlinearity

The damage in case 1 is induced through a 20% change in nonlinearity at a particular instant. From Figure 10, it is clear that the algorithm is able to perceive damage through the DSF even without the availability of the complete set of response. It is to be noted here that dof selected will have an impact on the detectibility limit. For the above case, the algorithm was able to detect changes in nonlinearity up to 20%. For the second case, 30% reduction in stiffness was induced in the fourth storey column at 31s and vibration responses from all the

floors except the second and fourth were made available as input to the algorithm. The results are as shown in Figure 11

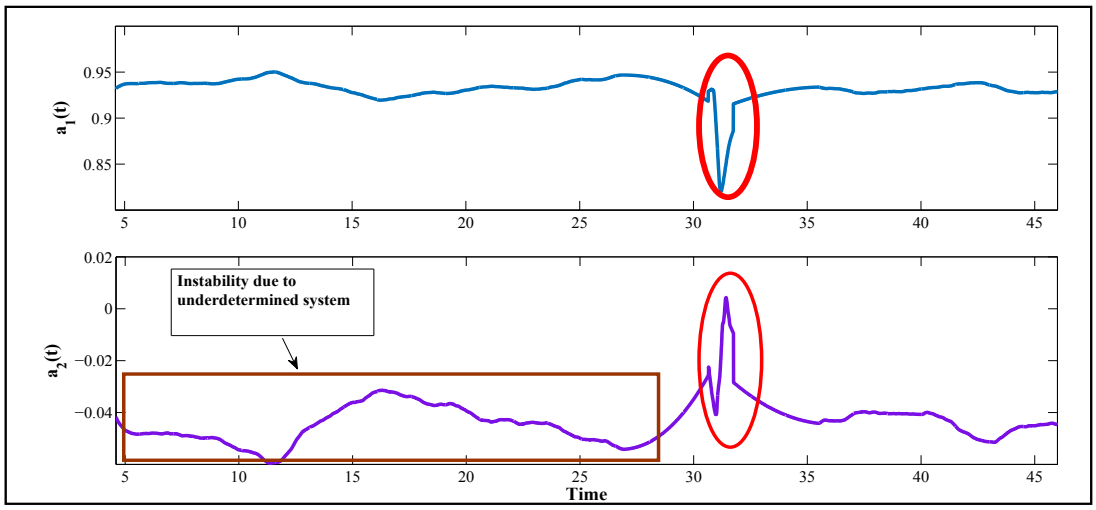


Figure 11: DSF for Underdetermined case 2- Local Damage, 30% change in stiffness

From the figures it can be seen that there is a lot of activity present before the instant of damage is attained. Albeit these instabilities, it can be safely concluded that the algorithm is well equipped to solve underdetermined system both for local damage and for global damage case scenarios.

## 6. Practical implementation studies

To substantiate the efficacy of the algorithm implemented online, three case studies have been presented:

1. An experimental model setup in a laboratory environment comprising of an aluminum beam excited by a ground motion, having a rubber strip attached to its free end.
2. A two-storey bench-scale model with a TMD is experimented with a Gaussian broad-band excitation to detect damage through a change in the values of optimal tuning parameters.
3. A full-scale study using recorded ambient and earthquake-excited responses obtained from UCLA factor building.

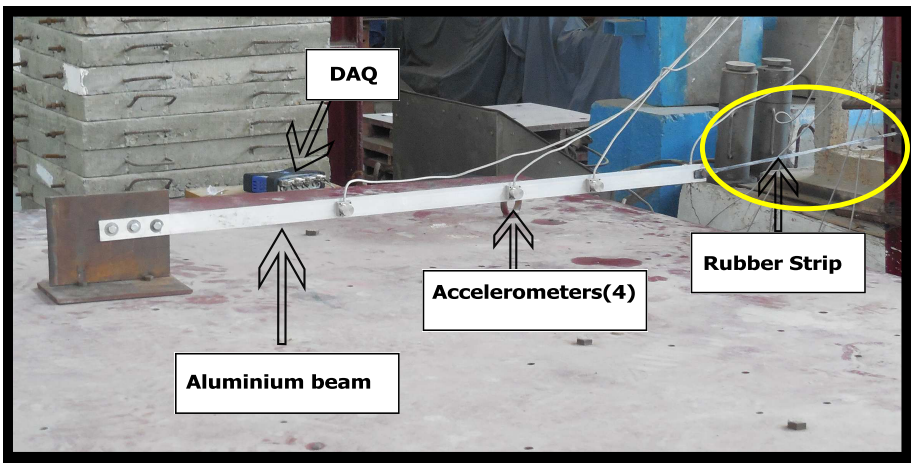


Figure 12: Details of the experimental setup

### *6.1. **Experimental Study***

In order to demonstrate the practical application of this method, an experimental setup is developed to simulate an online damage, and to validate the proposed real time damage detection algorithm. Figure 12 shows the setup consisting an aluminum beam of dimension $120cm \times 3.5cm \times 0.5cm$ fixed on a base plate which is drilled on top of a shake table (model no. Bi-00-300) ([50]). The base plate comprises of two metallic plates of dimension $23cm \times 15cm \times 1cm$ welded at right angles. A shake table of the following specifications is used to carry out the experiment: (i) table dimensions- $150cm \times 150cm$. (ii) payload capacity- $5tons$. (iii) peak velocity- $153cm/sec$. (iv) peak acceleration- $\pm 2.0$ g. (v) frequency range- $0 - 20$ Hz. The model is excited using a scaled Chi-Chi ground excitation and the response acceleration data are collected using QuantumX MX410 $HBM^{TM}$ Data Acquisition System (DAQ) at a sampling frequency 75 Hz. Honeywell accelerometers $TEDS$ by $HBM^{TM}$ are used to instrument the aluminum beam model at the following four positions: $1cm$, $30cm$, $47cm$ and $81cm$, from the free end, respectively. The output acceleration plot obtained from the sensors is shown in Figure 13. One end of the beam is clamped rigidly on a heavy steel platform; while a thin rubber strip of taut length 70cm attached to the free end of the beam provides nonlinearity to the entire setup.

The experiment is carried out by subjecting the aluminum beam to a scaled ground motion (1999 Chi-Chi ground motion, scaled to peak $0.3g$). In order to simulate a real time damage scenario, the rubber strip attached to the free end of the cantilever beam is snapped accurately at a fixed time instant, during the shaking motion

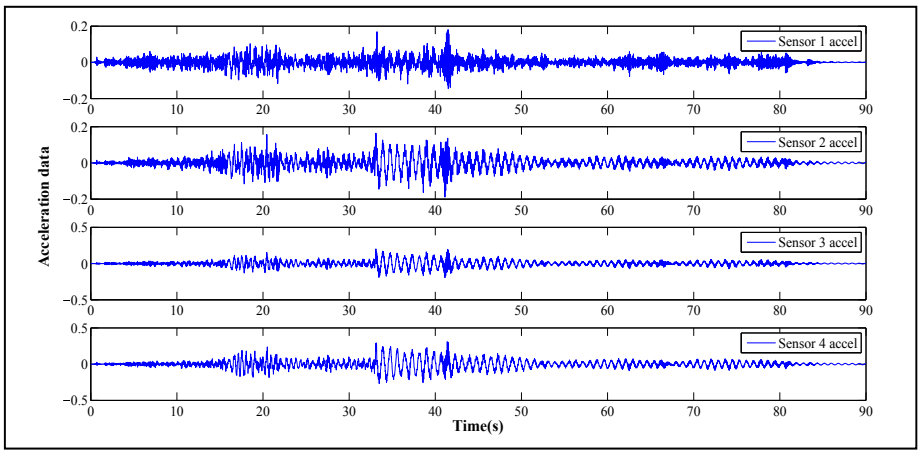


Figure 13: Output acceleration plot obtained from simulation

of the beam. The measurement of the instant of the snap is done using a stop watch and the entire experiment is recorded in the form of videos to assure accurate measurement of the instant. Damage ideally should be an instantaneous phenomenon, the action of snapping action as observed after repeated trials of experimentation takes at least 0.5 to 1 s. This small lag should be considered while calculating the damage instant. Hence, it is safe to assume that there is an error of 0.5 to 1 s in recording the time of damage. The recorded time of damage is then observed to be $33 \pm 1s$. The raw vibration data streaming in real time is acquired by the DAQ and then the proposed algorithm is applied. The instant of damage is well reflected by the plot of the DSF, which cannot be directly discerned from the raw acceleration data. It can be observed from Figure 14 that TVAR coefficient $a_1(t)$ shows a significant change in mean at 33s and $a_2(t)$ has significant activity at around the same time, indicating the occurrence of damage. The sudden change in level of sixth moment $\zeta_{a_i}(t)$ at 33s further adds to the evidence of damage occurrence at that point.

### *6.2. **Case study for de-tuning identification of tuned mass dampers***

In vibration control of structures, tuned mass dampers (TMDs) have been accepted as effective passive control device to alleviate unwanted vibrations in a flexible structure ([51, 52]). The dynamics and design of TMDs ([51]) involve the mechanism of mitigating the structural vibration by dissipating the undesirable vibration energy of the structure through the damping of the TMDs. De-tuning, resulting due to alterations of the primary and/ or TMD structure, incorrect design of forecasts, etc., lead to a substantial loss in the performance of TMDs,

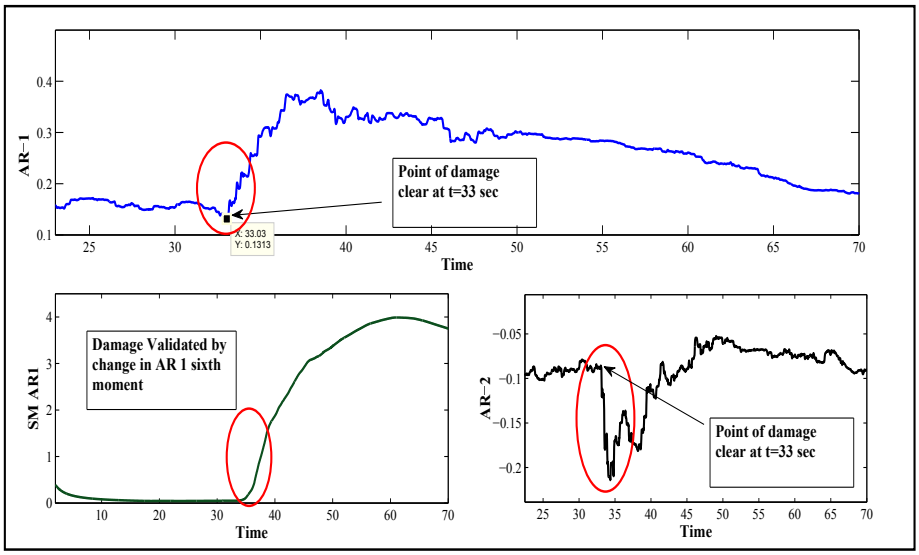


Figure 14: DSFs used for an experimental trial

which can be resolved by optimally tuning the natural frequency of the TMD to the structural natural frequency corresponding the mode to be controlled under a specified value of damping ([53]). Potential damages in a structure are related to the alterations in its primary properties, therefore, de-tuning of TMDs could practically be quantified as damage occurring in the structure. In order to understand de-tuning, it is instructive to express the equations of motion for a 2-dof structural system excited by stochastic disturbance, which is assumed to be Gaussian and white.

$$\begin{aligned} \mathbf{M}\ddot{\mathbf{X}} + \mathbf{C}\dot{\mathbf{X}} + \mathbf{K}\mathbf{X} - [\mathbf{k}(\mathbf{x} - \mathbf{X}) + \mathbf{c}(\dot{\mathbf{x}} - \dot{\mathbf{X}})] &= \mathbf{w} \\ \mathbf{m}\ddot{\mathbf{x}} + [\mathbf{k}(\mathbf{x} - \mathbf{X}) + \mathbf{c}(\dot{\mathbf{x}} - \dot{\mathbf{X}})] &= \mathbf{0} \end{aligned} \tag{30}$$

where $\mathbf{M}$, $\mathbf{C}$, $\mathbf{K}$ are the mass, damping, and stiffness coefficients of the primary structure, and $\mathbf{m}$, $\mathbf{c}$, $\mathbf{k}$ are the mass, damping, and stiffness coefficients of the TMD. $\mathbf{X}$ represents the displacement of the main mass with respect to the ground and $\mathbf{x}$ denotes the displacement of the TMD attached to the primary structure ([53]). For a general N-dof primary structure, the equations of motion for the $i^{th}$ mode when the TMD is present in the $j^{th}$ floor level can be written as (assuming a proportionally damped system)

$$\begin{aligned} \mathbf{M}_i\ddot{\mathbf{y}}_i + \mathbf{C}_i\dot{\mathbf{y}}_i + \mathbf{K}_i\mathbf{y}_i - \phi_{ij}[\mathbf{k}(\mathbf{x} - \mathbf{X}_j) + \mathbf{c}(\dot{\mathbf{x}} - \dot{\mathbf{X}}_j)] &= \mathbf{w}_i \\ \mathbf{m}\ddot{\mathbf{x}} + [\mathbf{k}(\mathbf{x} - \mathbf{X}_j) + \mathbf{c}(\dot{\mathbf{x}} - \dot{\mathbf{X}}_j)] &= \mathbf{0} \end{aligned} \tag{31}$$

where, the quantities $\mathbf{M}_i$, $\mathbf{C}_i$, $\mathbf{K}_i$ and $\mathbf{w}_i$ should be interpreted as corresponding to the $i^{th}$ mode. From equations

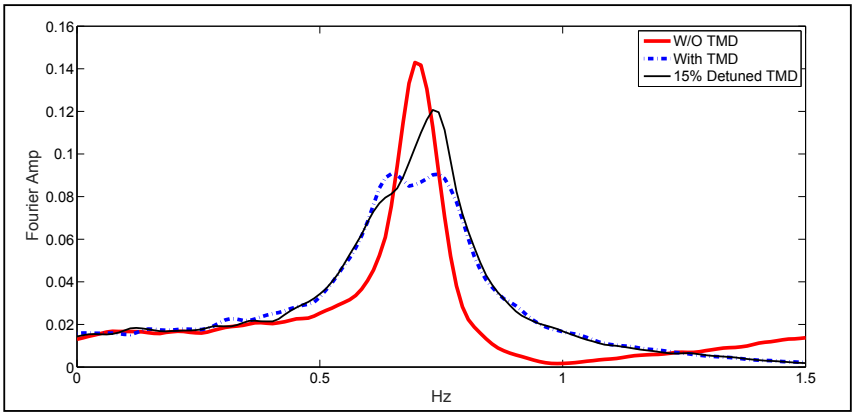


Figure 15: Tuned and de-tuned TMDs ($\alpha$= 0.85) (Raana and Soong, 1998, [51])

30 and 31, it can be observed that as long as $\phi_{ij}$ is normalized to unity for the $j^{th}$ floor location, the TMD design quantities obtained using equation 30 can be used directly to design a TMD corresponding to the $i^{th}$ mode ([51]). However, if the structure's $i^{th}$ mode shape vector is normalized with respect to its $j^{th}$ element, which corresponds to TMD location (i.e., the $j^{th}$ floor), $\phi_{ij}$ becomes unity and $\mathbf{X}_j(t) = \phi_{ij}\mathbf{y}(t) = \mathbf{y}(t)$. This implies that the expressions for calculating the steady-state $i^{th}$ modal response and damper response in a MDOF structure-TMD system will be exactly same as those for main mass and damper mass responses, respectively, in a SDOF structure-TMD system. The optimal TMD parameters are specified by its optimum mass ratio ($\mu_{opt}$), optimum frequency ratio ($f_{opt}$), and optimum damping ratio ($\xi_{opt}$). These quantities represent the ratio of the TMD parameters to the structure mass, modal frequency (to which the TMD is tuned to) and damping, respectively. For condition-assessment purposes, $\mu_{opt}$ is generally pre-defined as the mass ratio of the existing structure (i.e., $\mu_{opt}$= $\mu$). As documented in existing literature ([51, 52]), the values of $f_{opt}$ and $\xi_{opt}$ are determined as a function of the mass ratio and primary structure damping ratio ($\xi_p$). However, for de-tuning detection cases, the optimal design parameters of TMD that are of practical interest are the TMD stiffness ($k_{opt}$) and damping ($\xi_{opt}$) as de-tuning is primarily reflected by a change in the value of $k_{opt}$. Thus, a parameter $\alpha$ is used to express the TMD stiffness of the controlled system, evident by the relation $k_{TMD}$= $\alpha k_{opt}$, which quantifies the level of de-tuning in the system ([53]). A perfectly tuned condition implies that the value of $\alpha$ is unity, whereas $\alpha < 1$ or $\alpha > 1$, signify a de-tuned condition. A typical Fourier spectra of a de-tuned TMD is contrast to the perfectly tuned case and the absence of TMD case is shown in Figure 15. Figure 15 is obtained by incorporating the $\alpha$

parameter in Raana and Soong's model ([51]) and setting $\alpha = 0.85$. It is clear that de-tuning causes the Fourier amplitudes of the two closely spaced modes to be significantly different from each other. This phenomenon has been observed and reported in literature ([53, 54]).

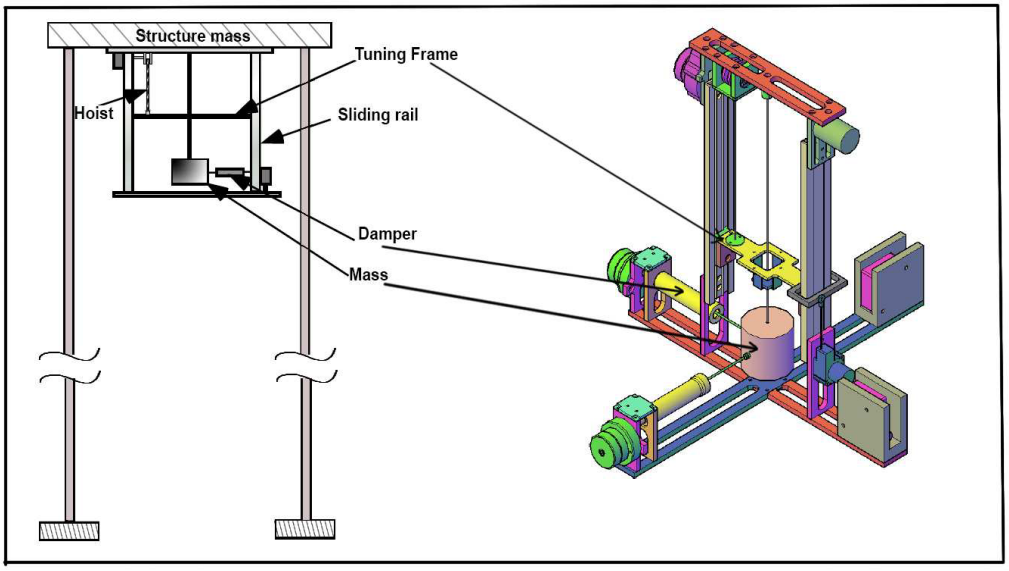


Figure 16: Schematic of the experiment setup (Hazra *et al*., 2010, [53])

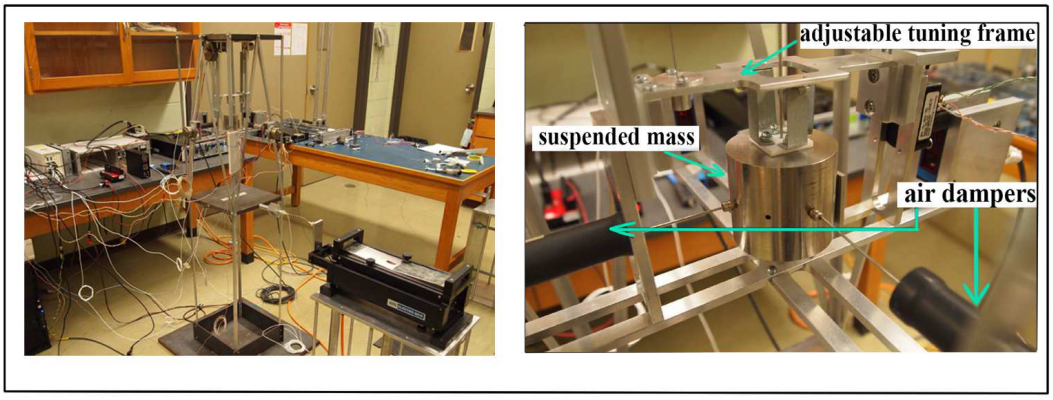


Figure 17: Experimental setup and instrumentation details

In order to demonstrate the practical applicability of the proposed damage detection method, the RPCA algorithm is implemented using acceleration data acquired from a bench-scale two-storey model, each with a floor weight of $140N$, with a pendulum TMD as shown schematically in Figure 16 ([53]). Flexural stiffness is provided by four $1.30cm$ aluminum equal angles, $130cm$ tall and $0.17cm$ thick. The lateral frequencies of

the bare structure (i.e., without TMD) are calculated as 2.6 and 3.5$Hz$ and the structural damping in both the lateral directions is assumed to be 2% critical in all the modes. The suspended mass is 1.5$kg$, which corresponds to a mass ratio of approximately 5%. The natural frequency of the pendulum is adjusted by sliding a tuning frame inside a rail and an air-damper is connected between the suspended mass and the rail assembly to provide a small amount of damping to the pendulum TMD. A broad-band excitation is commanded to an actuator as shown in Figure 17 which connected to the first floor level, and the accelerations are recorded using low-frequency accelerometers at the floor levels, in both the lateral directions. The sampling frequency is set to 100$Hz$ with a theoretically calculated optimal length of the pendulum to be 44$mm$ for the experimental setup, which will serve as a base-line to compare the re-tuned length.

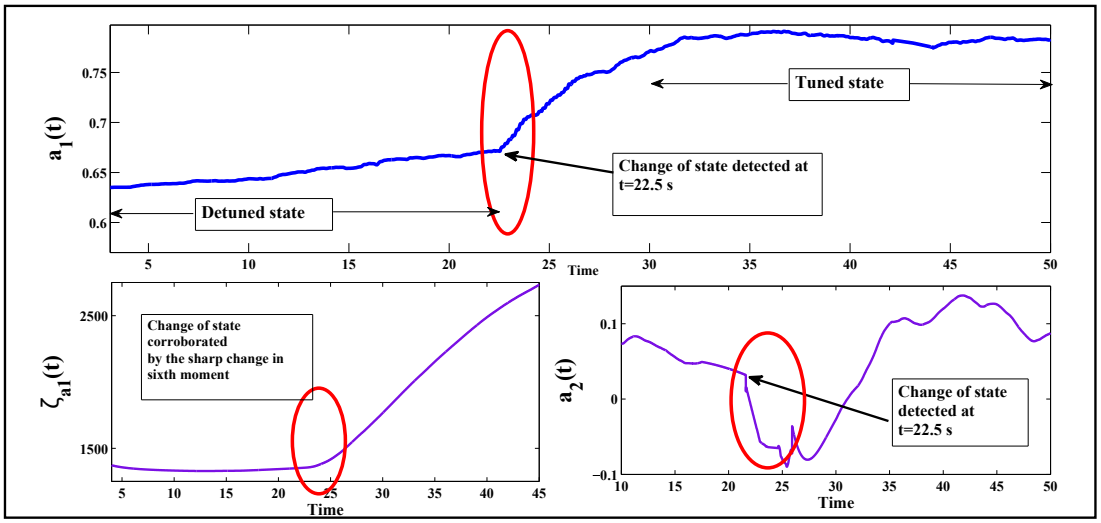


Figure 18: DSFs used for the TMD experiment

The tuning frame is adjusted first to a de-tuned configuration with an effective length of 30$mm$ and the acceleration response data are collected for the broad-band excitation case. Upon subjecting the structure to the excitation for a duration of 1 min., the effective length of the tuning frame was changed to the theoretical optimal length of 44$mm$ at around 23$s$ from the start of the excitation. The RPCA algorithm is applied on the accelerometer data mimicking a real-time application, in order to correctly capture the instant of damage. From Figure 18, it can be observed that the algorithm detects the damage instant online by tracking the change in TVAR coefficient ($a_1(t)$) at around 23$s$, showing a clear change in the level of $a_1(t)$, $a_2(t)$ and $\zeta_{a_i}$ at the instant of change of state. The figure clearly depicts the de-tuned state and the transition from the de-tuned state to

the tuned state after the instant of damage. It can be further observed that the plots of sixth moment and $a_2(t)$ deviate from the de-tuned state at around $23s$ which further substantiates the online damage detection by the RPCA algorithm.

### *6.3.* ***Case study for the UCLA factor building***

The proposed method is now applied to the ambient vibration data collected from the Doris and Louis Factor building (UCLAFB), which is a major facility located in the University of California campus in Los Angeles (UCLA). Designed and constructed in the late $1970s$, the 17 story 216.5 ft high UCLAFB is a $G + 15$ story structure (with basement and sub basement levels) that consists of special moment resisting steel frames (SMFs) supported by concrete bell caissons and spread footings. After the 1994 Northridge earthquake, the building was heavily instrumented with a network of 72 state-of-the-art Kinemetrics FB-11 uniaxial accelerometers at all the floor levels, which translates to 48 lateral and torsional channels of measurements. The array of sensors are converted to an equivalent array of $NS$, $EW$ and $\theta$ directional sensors lumped at the center of rigidity of each of the floors ([44]). This building is permanently instrumented, and the vibration data from this building is made available for researchers to examine through a remote data-base server. UCLAFB has been studied extensively in recent times mostly in the context of output only modal identification and the results are reported in some published works ([10, 44]). To test the efficiency and damage detection capability of the proposed algorithm, a combination of floor accelerations due to ambient data and data recorded during the event that occurred on September 28, 2004, 10:15 AM PDT, due to ground shaking originating (with M= 6.0 on the moment magnitude scale) from Parkfield, CA, are considered. The data is sampled at $100Hz$.

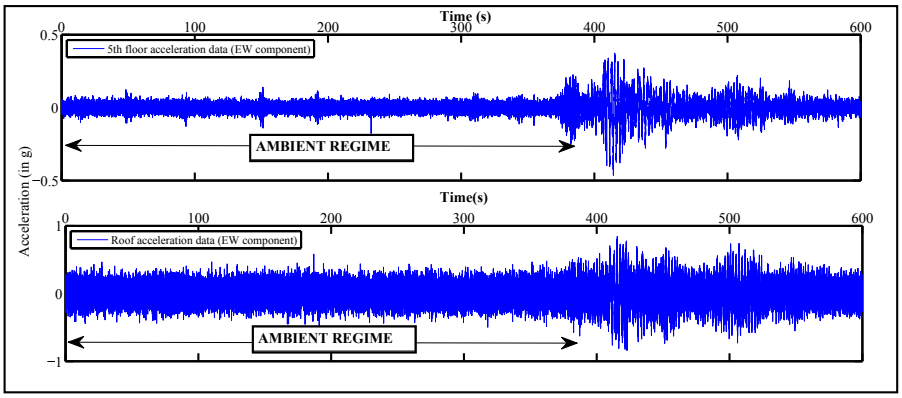


Figure 19: Roof and $5^{th}$ floor acceleration responses for UCLAFB in EW direction

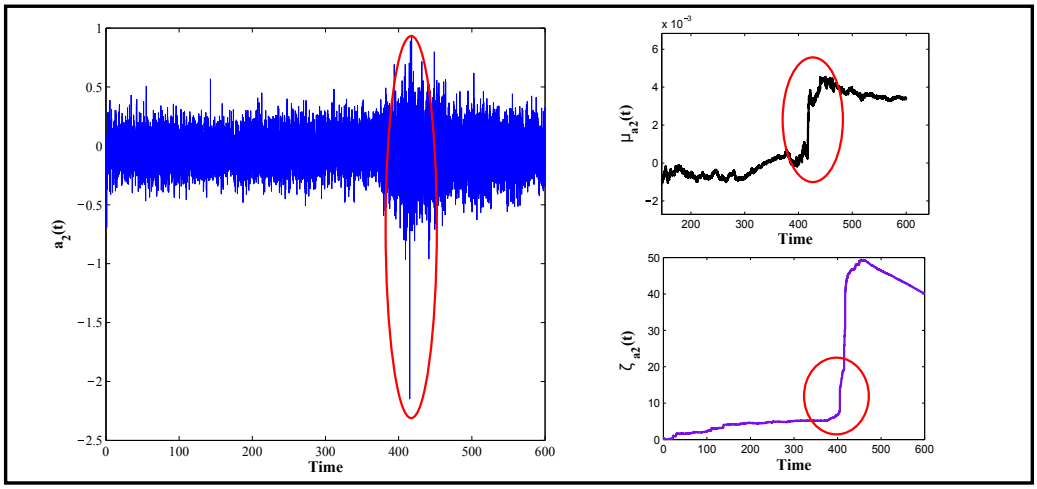


Figure 20: DSF for the UCLAFB

The acceleration data at roof and fifth floor in EW direction is shown in Figure 19. As seen from the figure, there is a considerable incidence of non-stationary activity in the vicinity of t=380$s$ which indicates the onset of the Parkfield earthquake (magnitude of Mw=6.0). The data prior to the occurrence of the earthquake corresponds to ambient vibration regime which is evident from Figure 19. All the 48 responses are utilized for online processing using the proposed RPCA algorithm and it has been observed that only the first eight modal responses are actively contributing to the vibration response. The instant of shaking as well as the instant of maximal structural change can be estimated from the DSF plots for the $N-S$ and $E-W$ components responses.

Upon a close analysis of the data, it could be easily inferred that the system response deviates from the ambient level at around t=380$s$, while the pronounced damage occurs at around t=410$s$. It is normal to expect these two instants to be different from each other because it takes a finite time for the structure to undergo significant changes (i.e. alteration of stiffness).

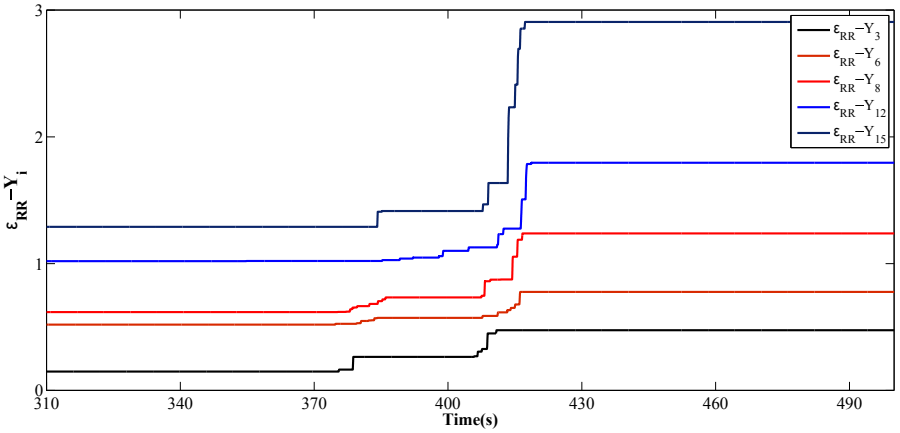


Figure 21: Residual error plots for floors of UCLA

Previous modal identification studies on UCLAFB [44] show 14.31%, 13.95%, 15.61%, 8.49%, 7.24%, 4.95%, 4.95%,30%, 6.5%, 4.75% percentage reduction in the values of identified frequencies between ambient vibration and earthquake data, which indicates significant global reduction in stiffness values. In the present context, global damage is expressed through percentage change in the average spatial RRE values (i.e. $\Delta\langle \varepsilon_{RR} - Y_i \rangle$ using equation 23) between the ambient and earthquake regimes corresponding to pre and post damage scenarios. Figure 21 shows the plot $\varepsilon_{RR} - Y_i$ for a few representative floors. It can be observed from the figure that $\varepsilon_{RR} - Y_i$ deviates from the ambient regime at around t=380$s$ and significantly in the vicinity of t=410$s$ indicating the occurrence of damage. The percentage change in post damage RRE and pre damage RRE (i.e. $\Delta\langle \varepsilon_{RR} - Y_i \rangle$) for each floor as shown in bardiagram Figure 22 which indicates the appearance of damage not only at a single floor but the system as a whole which corroborates to the previously mentioned results on modal identification [44].

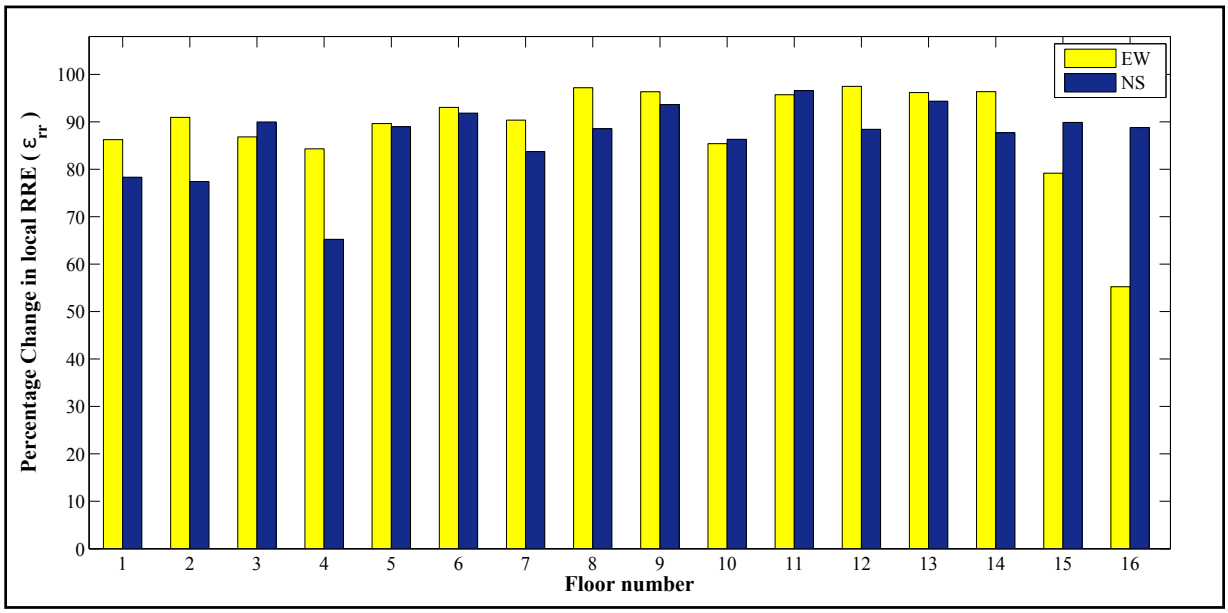


Figure 22: Bar diagram indicating percentage change in local RRE for EW and NS direction

## 7. Conclusions

A real time damage detection algorithm for vibrating systems based on recursive principal components in conjunction with TVAR model is presented. Recursive updates of the eigen subspace using rank one perturbation facilitated real time evolution of the principal components. Subsequent modeling of principal component explaining maximum variance makes the transformed response amenable to a low order TVAR model which is a key step of the proposed framework. The use of temporal RRE in conjunction with TVAR coefficients facilitated real time spatio-temporal damage detection. The proposed framework provided successful detection results for damages even up to 15% for the white noise excitation and up to 30% for the El Centro excitation case. Case studies have shown that the proposed algorithm is well equipped to detect damage when the number of sensors used to acquire data is reduced (i.e., for underdetermined systems), which is clearly an advantage while dealing with practical economics of health monitoring of real full-scale structures. The results show efficacy of the current framework to detect damage for underdetermined cases up to 20% change in the level of nonlinearity. The superiority of the RPCA based damage detection framework is clearly evident through the comparison with the traditional windowed batch PCA based framework, which is promising from a real time

damage detection standpoint. Presented case studies show that the proposed approach results in successful damage detection and works well even when used with both experimentally acquired data as well as large scale field data closely emulating practical scenarios.

## References


[1] C. R. Farrar, K. Worden, *An introduction to structural health monitoring*, Philosophical Transactions of the Royal Society of London A: Mathematical, Physical and Engineering Sciences 365 (1851) (2007) 303–315.

[2] D. Balageas, C.-P. Fritzen, A. Güemes, *Structural health monitoring*, Vol. 493, Wiley Online Library, 2006.

[3] J. B. Bodeux, J. C. Golinval, *Application of ARMAV models to the identification and damage detection of mechanical and civil engineering structures*, Smart Materials and Structures 10 (3) (2001) 479.

[4] K. Worden, *Structural fault detection using a novelty measure*, Journal of Sound and Vibration 201 (1) (1997) 85 – 101.

[5] S. W. Doebling, C. R. Farrar, M. B. Prime, et al., *A summary review of vibration-based damage identification methods*, Shock and vibration digest 30 (2) (1998) 91–105.

[6] C. R. Farrar, K. Worden, *Structural Health Monitoring: A Machine Learning Perspective*, John Wiley & Sons, Ltd, 2012.

[7] L. Balsamo, R. Betti, *Data-based structural health monitoring using small training data sets*, Structural Control and Health Monitoring 22 (10) (2015) 1240–1264, sTC-14-0113.R1.

[8] O. Salawu, *Detection of structural damage through changes in frequency: a review*, Engineering structures 19 (9) (1997) 718–723.

[9] K. Dziedziech, W. Staszewski, B. Basu, T. Uhl, *Wavelet-based detection of abrupt changes in natural frequencies of time-variant systems*, Mechanical Systems and Signal Processing 64 (2015) 347–359.

[10] F. Musafere, A. Sadhu, K. Liu, *Towards damage detection using blind source separation integrated with time-varying auto-regressive modeling*, Smart Materials and Structures 25 (1) (2015) 015013.

[11] V. H. Nguyen, J.-C. Golinval, *Fault detection based on kernel principal component analysis*, Engineering Structures 32 (11) (2010) 3683–3691.

[12] M. Lovera, T. Gustafsson, M. Verhaegen, *Recursive subspace identification of linear and non-linear Wiener state-space models*, Automatica 36 (11) (2000) 1639 – 1650.

[13] J. Hou, Åukasz Jankowski, J. Ou, *An online substructure identification method for local structural health monitoring*, Smart Materials and Structures 22 (9) (2013) 095017.

[14] D. P. Nguyen, M. A. Wilson, E. N. Brown, R. Barbieri, *Measuring instantaneous frequency of local field potential oscillations using the Kalman smoother*, Journal of neuroscience methods 184 (2) (2009) 365–374.

[15] W. Li, H. H. Yue, S. Valle-Cervantes, S. J. Qin, *Recursive PCA for adaptive process monitoring*, Journal of process control 10 (5) (2000) 471–486.

[16] A. Teughels, G. De Roeck, *Damage detection and parameter identification by finite element model updating*, Archives of Computational Methods in Engineering 12 (2) (2005) 123–164.

[17] *Civil structure condition assessment by {FE} model updating:: methodology and case studies* , Finite Elements in Analysis and Design 37 (10) (2001) 761 – 775.

[18] I. Behmanesh, B. Moaveni, *Probabilistic identification of simulated damage on the Dowling Hall footbridge through Bayesian finite element model updating*, Structural Control and Health Monitoring 22 (3) (2015) 463–483, sTC-13-0111.R2.

[19] K. N. Kesavan, A. S. Kiremidjian, *A wavelet-based damage diagnosis algorithm using principal component analysis*, Structural Control and Health Monitoring 19 (8) (2012) 672–685.

[20] Synchrosqueezed wavelet transform for damping identification, Mechanical Systems and Signal Processing 80 (2016) 324 – 334.

[21] S. Lin, J. N. Yang, L. Zhou, *Damage identification of a benchmark building for structural health monitoring*, Smart materials and structures 14 (3) (2005) S162.

[22] A. Kunwar, R. Jha, M. Whelan, K. Janoyan, *Damage detection in an experimental bridge model using Hilbert–Huang transform of transient vibrations*, Structural Control and Health Monitoring 20 (1) (2013) 1–15.

[23] V. Morovati, M. Kazemi, *Detection of sudden structural damage using blind source separation and time–frequency approaches*, Smart Materials and Structures 25 (5) (2016) 055008.

[24] A. Sadhu, B. Hazra, *A novel damage detection algorithm using time-series analysis-based blind source separation*, Shock and Vibration 20 (3) (2013) 423–438.

[25] M. De Oliveira, D. Inman, *PCA-based Method for Damage Detection Exploring Electromechanical Impedance in a Composite Beam*, Structural Health Monitoring 2015.

[26] M. Misra, H. H. Yue, S. J. Qin, C. Ling, *Multivariate process monitoring and fault diagnosis by multi-scale PCA*, Computers & Chemical Engineering 26 (9) (2002) 1281–1293.

[27] G. Kerschen, J.-C. Golinval, *Physical interpretation of the proper orthogonal modes using the singular value decomposition*, Journal of Sound and Vibration 249 (5) (2002) 849 – 865.

[28] L. Mujica, M. Ruiz, M. Pozo, J. Rodellar, A. Gaemes, *A structural damage detection indicator based on principal component analysis and statistical hypothesis testing*, Smart Materials and Structures 23 (2) (2014) 025014.

[29] I. Jolliffe, *Principal component analysis*, Wiley Online Library, 2002.

[30] A. Hot, G. Kerschen, E. Foltête, S. Cogan, *Detection and quantification of non-linear structural behavior using principal component analysis*, Mechanical Systems and Signal Processing 26 (2012) 104–116.

[31] F. Ding, T. Chen, *Identification of Hammerstein nonlinear ARMAX systems*, Automatica 41 (9) (2005) 1479–1489.

[32] S. Chen, S. Billings, P. Grant, *Recursive hybrid algorithm for non-linear system identification using radial basis function networks*, International Journal of Control 55 (5) (1992) 1051–1070.

[33] M. Z. Mistarihi, *Sensor-based Nonlinear and Nonstationary Dynaimc Analysis of Online Structural Health Monitoring*.

[34] M. Nigro, S. Pakzad, S. Dorvash, *Localized structural damage detection: a change point analysis*, Computer-Aided Civil and Infrastructure Engineering 29 (6) (2014) 416–432.

[35] G. E. P. Box, G. M. Jenkins, G. C. Reinsel, *Time Series Analysis*, John Wiley & Sons, Inc., 2008.

[36] H. Y. Noh, K. K. Nair, A. S. Kiremidjian, C. Loh, *Application of time series based damage detection algorithms to the benchmark experiment at the National Center for Research on Earthquake Engineering (NCREE) in Taipei, Taiwan*, Smart Structures and Systems 5 (1) (2009) 95–117.

[37] R. Yao, S. N. Pakzad, *Autoregressive statistical pattern recognition algorithms for damage detection in civil structures*, Mechanical Systems and Signal Processing 31 (2012) 355–368.

[38] B. Hazra, A. Sadhu, S. Narasimhan, *Fault detection of gearboxes using synchro-squeezing transform*, Journal of Vibration and Control (2016) 1077546315627242.

[39] G. Kerschen, J. C. Golinval, A. F. Vakakis, L. A. Bergman, *The method of proper orthogonal decomposition for dynamical characterization and order reduction of mechanical systems: an overview*.

[40] V. H. Nguyen, J.-C. Golinval, *Fault detection based on Kernel Principal Component Analysis* , Engineering Structures 32 (11) (2010) 3683 – 3691.

[41] B. Feeny, *On proper orthogonal co-ordinates as indicators of modal activity*, Journal of Sound and Vibration 255 (5) (2002) 805–817.

[42] B. Feeny, Y. Liang, *Interpreting proper orthogonal modes of randomly excited vibration systems*, Journal of Sound and Vibration 265 (5) (2003) 953 – 966.

[43] E. Kreyszig, *Advanced Engineering Mathematics: Maple Computer Guide*, 8th Edition, John Wiley & Sons, Inc., New York, NY, USA, 2000.

[44] B. Hazra, S. Narasimhan, *Wavelet-based blind identification of the UCLA Factor building using ambient and earthquake responses*, Smart Materials and Structures 19 (2) (2009) 025005.

[45] *Use of Wavelet-Based Damage-Sensitive Features for Structural Damage Diagnosis Using Strong Motion Data*, Journal of Structural Engineering 137 (10). doi:10.1061/(ASCE)ST.1943-541X.0000385.

[46] C. P. Ratcliffe, *Damage detection using a modified Laplacian operator on mode shape data*, Journal of Sound and Vibration 204 (3) (1997) 505–517.

[47] W. Lestari, P. Qiao, S. Hanagud, *Curvature mode shape-based damage assessment of carbon/epoxy composite beams*, Journal of intelligent material systems and structures 18 (3) (2007) 189–208.

[48] M. Gul, F. N. Catbas, *Statistical pattern recognition for Structural Health Monitoring using time series modeling: Theory and experimental verifications* , Mechanical Systems and Signal Processing 23 (7) (2009) 2192 – 2204.

[49] J. Ramallo, E. Johnson, B. Spencer Jr, *Smart base isolation systems*, Journal of Engineering Mechanics 128 (10) (2002) 1088–1099.

[50] K. Morita, M. Teshigawara, T. Hamamoto, *Detection and estimation of damage to steel frames through shaking table tests*, Structural Control and Health Monitoring 12 (3-4) (2005) 357–380.

[51] R. Rana, T. Soong, *Parametric study and simplified design of tuned mass dampers*, Engineering structures 20 (3) (1998) 193–204.

[52] J. P. Den Hartog, *Mechanical vibrations*, Courier Corporation, 1985.

[53] B. Hazra, A. Sadhu, R. Lourenco, S. Narasimhan, *Re-tuning tuned mass dampers using ambient vibration measurements*, Smart Materials and Structures 19 (11) (2010) 115002.

[54] J. Connor, S. Laflamme, *Structural motion engineering*, Springer, 2014.